Investigating Saporin-Conjugated Quantum Dots as a Microglia Depletion Strategy in the Substantia Nigra

By

Jeffrey Landrigan

A thesis submitted to the Faculty of Graduate and Postdoctoral Affairs in partial fulfillment of the requirements for the degree of

Master

in

Neuroscience

Carleton University

Ottawa, Ontario

Table of Contents

Abstract

Microglia depletion systems have been used to delineate the relationship between neuroinflammation and neurodegeneration, but come with many limitations. To sidestep these limitations, we employed a relatively new biological assay centered around saporin-conjugated quantum dots. Saporin is a type I ribosomal inhibitor protein which, when conjugated to a delivery molecule, has been used to selectively destroy targeted cells. Quantum dots are fluorescent semiconductor nanocrystals which are selectively taken up by microglia via clatherin-mediated endocytosis and can be used in conjunction with saporin to make a microglia-specific toxin (QD-SAP). Administration of QD-SAP at doses used in the literature caused the same microglial depletion observed *in vitro*, but in our *in vivo* studies also caused robust dopaminergic degeneration. This effect in not localized to the SNc, with administration of QD-SAP in the hippocampus (HPC) showing the same neuronal death. Interestingly, administration of QD-SAP in the HPC showed the same dopamine cell loss in the SNc as animals that received the toxin directly into the SNc. The reverse effect was not found. Together, these results provide intriguing new evidence of long-distance inflammatory propagation, and adds to the wealth of commentary on neuron-glia interactions in the substantia nigra.

Introduction

Parkinson's Disease (PD) is characterized by dopaminergic (DA) cell loss in the substantia nigra *pars compacta* (SNc) as well as α-synuclein (AS) aggregation, which leads to a host of motor and non-motor symptoms including bradykinesia, tremors and rigidity (Lang & Lozano, 1998). PD affects roughly 2% of the population, with a usual clinical onset between 60-65 years of age (Cummings, 1988; Hughes et al., 2000). Diagnosis occurs after approximately 50% of the nigrostriatal projecting DA neurons are lost and is primarily idiopathic, with less than 10% of cases being familial (Klockgether, 2004; Litteljohn et al., 2010). Current hypotheses attempting to explain neurodegeneration in the disease often postulate that genetic and environmental factors, whether primarily or secondarily, provoke long lasting "over-activation" of certain elements of the inflammatory immune system leading to neuronal death and dysfunction (Gao & Hong, 2008). Numerous factors, such as dysregulated protein expression/folding, endogenous oxidative stressors, environmental toxins, and genetic predisposition, come together in series and parallel to explain the chronic inflammation observed in PD (Béraud et al., 2013; James E. Galvin, 2006; Litteljohn et al., 2010; Lotharius & Brundin, 2002; Mastroeni et al., 2009).

Investigations of chronic inflammation in PD have often focused on the role of microglia, the resident inflammatory immune cell of the central nervous system (CNS) (Block, Zecca, & Hong, 2007). It has been suggested that alterations in microglial phenotype causes neuronal death through both chronic inflammation-oxidative stress factors along with a down-regulation of trophic support (Gao & Hong, 2008; Lull & Block, 2010). There are a plethora of factors that influence microglial reactivity, including environmental toxins, immune agents, microbial species and other various stressors (Béraud et al., 2013; Block et al., 2007; Erny et al., 2015). It has been generally accepted that the combination of such insults, together with some genetic vulnerability

factors ultimately contribute to the development of PD (Litteljohn et al., 2010). Indeed, exposure to environmental stressors have been implicated in microglial "hyper-reactivity", including chemical, microbial or heavy metal toxins (Gao & Hong, 2008). Moreover, modified or aggregated proteins such as a-synuclein rich Lewy bodies, or damaged neurons themselves can likewise serve as activation triggers for microglia (Gao & Hong, 2008).

In the present thesis, we were interested in selectively targeting microglia within the SNc using saporin, a ribosomal inhibitor protein, which has previously been shown to deplete microglia (Minami et al., 2012). As will be discussed in subsequent sections of this thesis, we hope to develop a novel method of imaging and manipulating SNc microglia using saporin and quantum dot technology in a hope of better understanding microglial involvement in dopaminergic neuronal death, as occurs in PD.

Microglia and neuroinflammation

Microglia normally provide neuronal support by the release of trophic factors, including brain derived neurotrophic factor (BDNF), as well as by clearing any cellular debris or metabolic by products through phagocytosis (Block et al., 2007). During this relatively quiescent resting state, microglia have immobile ramified morphology characterized by a small cell body with long, thin processes that extend out into the extracellular milieu. These processes possess pathogen-associated molecular pattern (PAMP) receptors or damage-associated molecular pattern (DAMP) receptors, allowing them to detect and deal with any microbial or other invaders (Gehrmann, Matsumoto, & Kreutzberg, 1995). Damaged or stressed cells release ATP into the extracellular space, which microglia can detect and follow in order to remove debris (Davalos et al., 2005). While removing cellular debris, microglia will also extend their processes to shield healthy

neurons from dying tissue, as well as release chemokines to recruit neighboring microglia, and release inflammatory cytokines to induce further microglial proliferation (Gao & Hong, 2008).

Neuroinflammation is a normally protective response orchestrated by microglia—and aided by astroglia—that serves to mobilize the central immune system, remove noxious stimuli, and begin regenerative processes (Gao & Hong, 2008). Microglia release a wide range of pro- and anti-inflammatory cytokines including interferons (IFN), interleukins (IL), and tumor necrosis factors (TNF) (Clausen et al., 2008). Proinflammatory cytokines typically act through three pathways: (1) Nuclear Factor κ B (NFκB), (2) c-Jun N terminal kinase (JNK), or (3) janus kinase (JAK) and signal transducer and activator of transcription (STAT) (Litteljohn et al., 2010).

TNF-α and IL-1β stimulate the phosphorylation and subsequent degradation of inhibitor factor κ (IFκ), which normally arrests NFκB—the now free NFκB translocates to the nucleus where it initiates expression of numerous apoptotic and inflammatory machinery such as cyclooxygenase-2 (COX-2). These factors can lead to the generation of reactive oxygen species (ROS), which can damage DNA and provoke lipid peroxidation (Hayley, Mangano, Strickland, & Anisman, 2008). Similarly, IL-6, IL-10, and IFN-γ promote the activation of JNK and JAK/STAT pathways through a series of protein phosphorylation events, ultimately leading to the induction of inducible nitric oxide synthase (iNOS), nicotinamide adenine dinucleotide phosphate (NADPH) oxidase, and COX-2, which all lead to neuronal death (Litteljohn et al., 2010). In essence, microglia normally work to detect and destroy dying or dysfunctional cells while simultaneously protecting healthy cells (Streit, Walter, & Pennell, 1999).

Microglial inflammation is categorized as primary or secondary based on the originating signal. Primary inflammation is distinguished from secondary inflammation by the presence of PAMPs or DAMPs of non-neuronal origin, such as bacteria and viruses. Secondary inflammation

(sometimes referred to as sterile inflammation) is characterized by neuronal lesions due to trauma, genetic predisposition or environmental toxins (Gao & Hong, 2008). Upon activation, microglia change from a ramified to an amoeboid shape and rapidly phagocytose any pathogens or dying cells (Hanisch & Kettenmann, 2007; Kreutzberg, 1996; Ransohoff & Perry, 2009). It should be underscored that this is a highly simplified view, as microglia actually exist across a spectrum of phenotypes (Wake, Moorhouse, Jinno, Kohsaka, & Nabekura, 2009).

Microglia and neuronal support

Microglia also provide support through the secretion of the trophic factors such as brain-derived neurotrophic factor (BDNF), glial cell line derived neurotrophic factor (GDNF) nerve growth factor, and neurotrophin-3 (Peterson & Nutt, 2008; Suzuki, Imai, Kanno, & Sawada, 2001). GDNF has been shown to be neuroprotective and regenerative through direct influences on neurons and through activation of microglia (Boscia et al., 2009; Peterson & Nutt, 2008). Similarly, BDNF is neuroprotective and plays a supportive role to neurons through its influence on learning-dependent synapse formation (Paolicelli et al., 2011; Parkhurst et al., 2013).

Microglia mediate synaptic functioning, with their processes extending to physically contact neurons to shape firing patterns (Schafer et al., 2012; Wake et al., 2009). Upon detection of dysfunctional firing, microglia will phagocytose the presynaptic input, thereby eliminating the faulty synapse (Schafer et al., 2012). In line with this, a recent report found that reductions in microglia-mediated synaptic pruning lead to weak synaptic transmission (Zhan et al., 2014). Interestingly, it has been suggested that synaptic pruning is only important during early postnatal development and that microglia-mediated synapse formation in adulthood is more important than synapse elimination (Parkhurst et al., 2013). However, a recent report has shown that that displacement of inhibitory synapses from cortical neurons by microglia increases synchronic

neuronal firing and subsequent calcium-mediated pro-survival gene transcription in adult mice; suggesting that both synapse formation and removal are vital for proper neuronal support regardless of age (Chen et al., 2014).

Genetic and pharmacological manipulation of microglia

Microglia depletion systems use genetic or pharmacological treatments to delineate the role of microglia in neurodegenerative, neuroinflammatory, or other conditions (Waisman, Ginhoux, Greter, & Bruttger, 2015). Genetic deletion models target key genes in microglia development such as, PU.1, CSF-1R, and TGF-β; however, their use is limited as these mice rarely survive development and have a host of central and peripheral deficits (Butovsky et al., 2014; Ginhoux et al., 2010; Kierdorf et al., 2013; McKercher et al., 1996; Scott, Simon, Anastasi, & Singh, 1994). For example, studies using cx3cr1$^{-/-}$, CR3$^{-/-}$, and DAP12$^{-/-}$ mutants revealed that manipulation of microglial activity affected outgrowth of DA axons, suggesting that microglial dysfunction affects forebrain connectivity (Squarzoni et al., 2014). While useful for studying development, it is difficult to adequately mimic the pathogenesis of diseases like PD, which typically begins later in life.

Conditional gene knockout techniques have been used to sidestep developmental deficits in genetic deletion (Waisman et al., 2015). One of the main techniques used was refined throughout a series of experiments initiated by Heppner *et al.*, who in 2005 generated a mouse line expressing the suicide gene thymidine kinase (TK) under the myeloid-specific promoter CD11b. Administering ganciclovir (GCV) to these animals eliminates any CD11b^{+} cells (2005), thus effectively depleting microglia. However, these mice experienced the same premature death as the other genetic deletion models. It was then discovered that intra-cerebroventricular administration of GCV under the same paradigm as Heppner *et al.* led a 90% depletion of microglia after 2 weeks

(Grathwohl et al., 2009). Nonetheless, treatment frequently led to death at 4 weeks, and the injections locally perturbed the blood-brain barrier (BBB), allowing peripheral immune cells entry into the CNS (Grathwohl et al., 2009).

Other knockout techniques use tamoxifen-inducible cre-recombinase Cx_3Cr1^{creER} mice, which takes advantage CX_3CR1, a fractalkine receptor abundantly expressed on microglia (Parkhurst et al., 2013; Yona et al., 2013). When crossed with Cre-inducible diphtheria toxin receptor (iDTR) transgenic mice, administration of diphtheria toxin can cause >90% selective ablation of microglia (Buch et al., 2005). Microglia depletion using Cx_3Cr1^{creER}-iDTR mice is short lived, with the majority of the cells repopulated within 5 days (Bruttger et al., 2015). If warranted, bone marrow (BM) grafting can be added to this technique, which results in the repopulation of microglia from the BM rather than from the 5-10% of surviving microglia (Bruttger et al., 2015). Compared to the $CD11b^+$ technique, this method circumvents the issue of infiltrating peripheral myeloid cells (Waisman et al., 2015). Microglia are normally long-lived self-renewing cells, whereas peripheral myeloid cells are short lived; therefore, if enough time elapses between tamoxifen treatment and creation of Cx_3Cr1^{creER}-iDTR mice, only the long-lived microglia will continue to express Cx_3Cr1^{creER} (Bruttger et al., 2015; Goldmann et al., 2013). Thus, microglia but no other myeloid cells will be affected upon exposure to diphtheria toxin. Nonetheless, as both BM grafting and tamoxifen administration has immunomodulatory effects beyond microglia, further characterization of the immune phenotype generated by these mutated animals should be conducted (Waisman et al., 2015).

Agents such as saporin (SAP)-conjugated macrophage antigen complex-1 (MAC-1) and the CSF-1R inhibitory drug, PLX3397, have also been used to pharmacologically deplete microglia in mice (Elmore et al., 2014; Heldmann, Mine, Kokaia, Ekdahl, & Lindvall, 2011).

PLX3397 is a colony stimulating factor (CSF) 1 receptor and c-Kit kinase inhibitor, which results in ~99% elimination of microglia when administered through chow (Elmore, Lee, West, & Green, 2015). Upon cessation of drug delivery, microglia rapidly repopulate, completely recovering in ~5 days for PLX3397 and <14 days for MAC-1-SAP (Elmore et al., 2015; Montero, González, & Zimmer, 2009). Importantly, elimination of microglia had no significant effect on astrocytes, neurons, or oligodendrocytes (Elmore et al., 2014). In contrast to MAC-1-SAP, PLX3397 microglia repopulation has been shown to occur solely due to microglia proliferation with no supplementation from infiltrating peripheral myeloid cells (Elmore et al., 2014). Currently, the only method of delivery has been through chow, resulting in global ablation of microglia in the CNS and moderate effects on the PNS (Elmore et al., 2014). To date, no investigations have administered PLX3397 directly into the CNS of mice or rats.

MAC-1 ($CD11b^+$) is a receptor abundantly expressed on microglia and saporin is a type I ribosomal inhibitor protein; when combined, MAC-1-SAP is internalized into $MAC1^+$ myeloid cells, wherein saporin inhibits protein translation (Bagga, Hosur, & Batra, 2003; Montero et al., 2009). MAC-1-SAP is highly selective, with $MAC\text{-}1^-$ cells being unaffected by treatment (Heldmann et al., 2011; Imai & Kohsaka, 2002). Administration of MAC-1-SAP provokes a 24h inflammatory response which is most likely due to cytokine release from dying microglia undergoing apoptosis (Yao et al., 2016). Mixed cell-culture studies have provided evidence that MAC-1-SAP had no significant effect on neurons or astrocytes (Montero et al., 2009).

Repeated intraperitoneal injection of MAC-1-SAP was reported to be protective against the neurotoxicant, ibotenic acid (Dommergues, Plaisant, Verney, & Gressens, 2003). As it is not known whether MAC-1-SAP can cross the BBB, it has been suggested that this result was due to the attenuation of infiltrating leukocytes, rather than depletion of microglia (Dommergues et al.,

2003). Indeed, MAC1 is important for cell-cell adhesion and the process of leukocytes crossing the BBB (Takeshita & Ransohoff, 2012). A recent study in which MAC-1-SAP was administered intra-thecally reported local disruption in the blood-spinal cord barrier, coupled with increased mRNA expression of inflammatory cytokines (Yao et al., 2016). Nonetheless, from this data we cannot conclude whether ibotenic acid injury was reduced due to MAC-1-SAP-induced decreases in microglial populations or attenuation of leukocyte infiltration.

The use of saporin for microglial ablation in PD models using MAC-1 and quantum dot delivery mechanisms

Given the severe limitations already mention with regards to microglial depletion methods, the purpose of this investigation is to characterize the novel application of saporin together with quantum dot technology as a means to manipulate and visualize microglia. We are particularly interested in using this tool for further assess inflammatory mechanisms in PD.

As already alluded to, saporin is a type 1 ribosomal inactivating protein (RIP) (Bagga, Hosur, et al., 2003). RIPs define a class of toxic proteins which have *N*-glyocosidase enzymatic activity, which predominantly targets ribosomal machinery, attenuating protein synthesis leading to cell death (Gilabert-Oriol et al., 2014). There are three types of RIPs: Type I are characterized by an A chain, which houses the *N*-glyocosidase catalytic machinery, but lacking a B chain, which facilitates cellular entry through interaction with galactose residues on the cell membrane. Type II contain both chain A and B. Type III are a rare case and are characterized as a protein evolutionarily related to jasmonate-induced protein from barley (Gilabert-Oriol et al., 2014). Type I RIPs are considered less toxic than type II, due to their inability to easily enter a cell; however, they do become highly toxic when they are bound to a carrier that can mediate their transport inside the cell (Stirpe, 2004).

Saporin-6, the most abundant isoform, contains two catalytic domains: the first is the RNA-*N*-glycosidase domain responsible for ribosomal inhibition and the second is a DNA inter-nucleosomal fragmentation domain (Bagga, Seth, & Batra, 2003). The resultant structure of saporin makes it significantly more toxic than other RIPs in terms of both LD50 and half-life (Blakey et al., 1988). Indeed, compared to ricin, one of the most common type II RIPs, saporin is 6 to 30-fold more toxic even whilst binding 5-fold less (Blakey et al., 1988). Additionally, when mice were given median lethal doses of ricin or saporin, blood levels fell below toxic concentrations after 4 hours for ricin, but remained lethal after 48 hours for saporin (Blakey et al., 1988). These characteristics, combined with stability in high uric acid (4 M) and temperature (55°C) makes saporin a prime candidate for the generation of immunotoxins (Santanché, Bellelli, & Brunori, 1997).

To create an immunotoxin specific to microglia, saporin may be conjugated to MAC-1 or a quantum dot (QD) (Minami et al., 2012; Montero et al., 2009). MAC-1 is a receptor found on myeloid cells and has potential to selectively ablate microglia in the brain. In an MPTP model of PD, MAC-1 was found to mediate reactive microgliosis and progressive dopaminergic neurodegeneration (Hu et al., 2008). The use of MAC-1-SAP has the advantage then of specifically targeting the myeloid cells implicated in MPTP induced parkinsonism. Indeed, MAC-1-SAP has already been used to locally ablate microglia intra-thecally, and MAC1 expressing microglia have been implicated in PD (Yao et al., 2016).

Quantum dots are fluorescent semiconductor nanocrystals comprised of a metallic core and semiconductor shell—the dot is typically composed of a cadmium selenide (CdSe) core and a zinc sulfide (ZnS) shell—and can be used to selectively deliver saporin to microglia (Jaiswal & Simon, 2004). Compared to organic fluorophores used on MAC-1, QDs have the advantage of having a

narrow emission spectrum, which reduces spectral overlap, allowing for more fluorophores to be distinguished simultaneously (Jaiswal & Simon, 2004). Additionally, they show much higher bio- and photo-stability (Jaiswal & Simon, 2004). *In vivo,* QDs can be detected with fluorescent imaging for at least 4 months (Ballou, Lagerholm, Ernst, Bruchez, & Waggoner, 2004), and photobleaching using a 50-mW light found QDs to remain stable after 14h, which is significantly better than organic fluorophores such as fluorescein, which completely photobleach in less than 20 min (Jaiswal & Simon, 2004).

One of the main determinants of whether a QD enters a cell is its size—in most cases, QDs need to be conjugated to a peptide that facilitates their entry into a cell (Jaiswal & Simon, 2004). Indeed, unconjugated quantum dots do not entire neurons (Vu et al., 2005). Conveniently, unconjugated QDs do enter microglia (Minami et al., 2012). The size of QD does affect their ability to enter microglia, with QDs that emit at 655nm wavelengths being taken up most readily (Minami et al., 2012). Finally, QDs are not harmful to cells at relevant doses, with concentrations of up to 1μM causing no "ill effects" (Voura, Jaiswal, Mattoussi, & Simon, 2004).

Biotinylated saporin can be conjugated to streptavidin-linked CdSe/ZnS QDs (QD-SAP) for selective delivery into microglia. So far, only one experiment has been performed using QD-SAP (Minami et al., 2012). In this study, using cell culture and stereotaxic injections, QD-SAP cellular entry was found to require clatherin-mediated endocytosis involving macrophage scavenger receptor 1 and mannose receptors, both of which are specific to microglia (Minami et al., 2012). Importantly, in cortical cultures with MAP2-positive neurons, GFAP-positive astrocytes, and CD11b-postive microglia, only microglia took up the QDs (Minami et al., 2012). Finally, QD-SAP mediated microglia ablation had no effect on number or morphology of neurons

or astroglia, and uptake of QDs themselves did not result in any cytokine release or other signs of inflammation (Minami et al., 2012).

In short, MAC-1-SAP and QD-SAP are both strong candidates for use as microglial ablation systems. Compared to genetic strategies, these systems cost less are more specific to microglia, and have fewer side effects (Waisman et al., 2015). Compared to the other main pharmaceutical agent, PLX3397, both targeting systems have been used successfully for the local ablation of microglia rather than global ablation as is evident with PLX3397. Thus, MAC-1-SAP and QD-SAP are logical choices for targeting SNc microglia and subsequent assessment of dopaminergic neuronal survival/viability. Indeed, we believe MAC-1-SAP and QD-SAP can be used in PD models to better understand the role of chronic inflammation and reactive microgliosis in the disease. Many factors, such as α-synuclein, genetic predisposition, environmental toxins, and endogenous oxidative stressors have been implicated in the pathogenesis of PD, and all of these factors have been shown to influence inflammatory processes (Béraud et al., 2013; Chu & Kordower, 2015; Couch, Alvarez-Erviti, Sibson, Wood, & Anthony, 2011; J. E. Galvin, Lee, & Trojanowski, 2001; James E. Galvin, 2006; Litteljohn et al., 2010; Lotharius & Brundin, 2002; Mastroeni et al., 2009).

The present thesis involves a series of experiments that will characterize the effects of local infusion of MAC-1-SAP and QD-SAP on SNc microglia and neurons. Through these experiments, we will be able to characterize, for the first time, the effect of selectively targeting microglia with the saporin toxin *in vivo* using wild-type animals and in conjunction with QDs and MAC1. This will help determine if these two depletion systems are relevant for the study of chronic reactive microgliosis in PD.

Methods

Animals

102 male C57Bl6/N mice (8-10 weeks of age upon delivery) were purchased from Charles River. All mice had free access to food (Ralston Purina mouse chow) and were individually housed in standard mouse cages (27X21X14cm polypropylene cages) in the same room. The temperature of the room was 23ºC. Body weight was measured weekly.

Experimental Groups

A pilot study was performed with a subset of the animals to determine if the surgical and histochemical procedures reported in the literature were replicable. To this extent, a pilot cohort (n=18) was separated into three groups as follows: 1. Surgical Controls (Saline) 2. Standard QD-SAP (0.025µM) and 3. Standard MAC-1-SAP (2.0µg). This study assessed which toxin method had the most robust impact on microglia.

After analysis of the pilot tissue as described in the histochemistry and stereology sections below, another cohort of animals (n=30) was experimentally run. We chose the QD-SAP toxin over MAC-1-SAP given that our data from the pilot trial indicated that both toxins had similar effects on microglia but QD-SAP has the added benefit of autofluoresence. Hence, mice were divided into 3 different treatments (n=10) as follows: 1. Surgical Controls (Saline) 2. Standard QD-SAP (0.025µM) and 3. Low QD-SAP (0.0125µM).

Another, final experiment (tissue is still being processed, but preliminary data is presented here) was conducted to understand the temporal effect of QD-SAP as well as potential regional effects, and also to further titrate the dose in the SNc to 0.005µM. To this extent, 54 mice were divided into 9 treatment groups (n = 6, Region-Dose-Experimental Endpoint): 1. SNc High 1 Day, 2. SNc High 2 Day, 3. SNc High 7 Day, 4. SNc Very Low 7 Day, 5. HPC High 7

Day, and 6, 7, 8, and 9 are unconjugated QD controls for SNc 1, 2, and 7 Day and HPC 7 Day QD-SAP groups. Animals were given the high dose of QD-SAP to be increase comparability to the literature. In the past experiments, animals receiving the high dose of QD-SAP in the SNc reached humane euthanasia endpoints. If this happens to any animal in any of the groups, the entire group will be euthanized at the same time to make the results comparable, and to identify what is happening in the brain at the onset of the circling behavior.

Surgery

MAC-1-SAP was purchased from Advanced Targeting Systems (IT-06). MAC-1-SAP powder was dissolved into PBS to create a 1.0µg/µl MAC-1-SAP solution. Water-soluble CdSe core ZnS shelled QDs coated in streptavidin with an emission maxima of ~585 nm was purchased from ThermoFisher Scientific (Q10113MP). Biotin-labelled saporin chicken polyclonal was purchased from Advanced Targeting Systems (BT-17AP). The avidin-biotin affinity was used to conjugate saporin to the quantum dots**.** 2µl of QDs (1µM) were mixed with 2µL of biotinylated saporin (56µM) and 76µL of phosphate buffer solution was added. 40µL of this solution was extracted and mixed with 40µL of PBS to create the low dose toxin solution. Solutions were incubated at room temperature for 1 hour on a Belly Dancer from Fisher Scientific before surgery.

Animals were anesthetized with 5% isoflourane and administered Tramadol at 2.5mg/kg at a concentration of 2.5 mg/ml and 0.3 mL sub-cutaneous saline. Animals were secured in the Kopf Instruments Model 940 stereotax frame using xylocaine (2% lidocaine hydrochloride topical anaesthetic, AstraZeneca) coated earbars. A small, 1.5cm incision was made in the centre of the skull and a 1.5mm diameter hole was drilled in the skull at x = 1.4mm and y = 3.14mm for the SNc, and x=-1.7mm, y=-2.1mm, and z=-2.0mm relative to bregma over the left hemisphere.

A 22 guage injector is used to infuse 2µL of either saline QD-SAP, or MAC-1-SAP directly above the SNc 4mm below the surface of the skull. A Harvard Apparatus picopump 11 double syringe pump was used to ensure a constant infusion over 4 minutes. The injector was left in place for 5 minutes after the infusion to allow the QD/Saline to absorb into the tissue before slowly being removed. The hole in the skull was filled with Bone Wax® before suturing. To recover from the anesthesia the animals were given 100% 02 for 15 seconds before being removed from the stereotax. Surgeries typically last 25 minutes

Behavioral testing

1) Undisturbed locomotion will be continuously evaluated in the home cage using a Micromax beam-bream apparatus (AccuScan, CA) equipped with 16 photocells interfaced into a digital analyzer. Testing durations will be 16 hours, 4 hours of acclimatization and 12 hours of recording. Recording takes place overnight from 2000 to 0800 hours.

3) Balance and coordination will be evaluated using the rotarod apparatus. The rotarod consists of an enclosed 8cm long rubber coated rod suspended 30cm above an infared beam. The animal is placed on the rod which is rotated with constantly increasing speed from 4rpm up 44rpm over 5 minutes. When the mouse falls, the beam is broken and the computer records the velocity and time and which the animal fell.

All animals will undergo a baseline MMx run one week after arrival (Acclimation period). The following day (Day 1 of the experiment) they will undergo stereotaxic surgery to infuse 2uL of: Saline, 0.025uM quantum dots or 0.015uM quantum dots. The animals will be allowed to recover for 3 days receiving post-operative care. On experimental day 5 animals will undergo a MMx test. On day 11 they will begin rotorod training as cumulating in the rotorod,

and MMX tests on day 13. The morning of day 14 half of the animals from each treatment group (5 each) will be perfused for immunohistochemical analysis while the other 5 per group are rapidly decapitated for unfixed tissue collection.

Western Blot

Tissue punches will be collected from the PFC, SNc, and striatum to detect levels of immune activation via Cx3Cr1 (Sigma-Aldrich, Cat #SAB3500204) and Wave2 (Cell Signaling, Cat #3659S). Protocol for western blot staining was adapted from Litteljohn et al. (2011). Primary antibodies for Cx3Cr1 and Wave2 (1:300) will be used and β-actin (1:20000, Sigma-aldrich, Cat #WH0000060M1) applied as a loading control. Following our previous procedures (Mangano & Hayley, 2009), tissue punches will be diluted in an extraction buffer (5.0 M NaCl, 0.5 M EDTA, 100 mM EGTA, 1M DTT, 50% glycerol, 0.1M PMSF, 10mg/ml leupeptin, 5 ug/ml aprotinin, 1 M -glycerophosphate, 0.5 M NaF, and 100 mM Na-orthovanadate), sonicated, centrifuged at 14000 rpm, (15 min) and supernatant assessed for protein concentration using a BioRad protein assay.

Whole cell lysates were homogenized in ice-cold Radio Immuno Precipitation Assay (RIPA) buffer [50 mM Tris (pH 8.0), 150 mM sodium chloride, 0.1% sodium dodecyl sulphate (SDS), 0.5% sodium deoxycholate and 1% Triton X-100] mixed with 1 tablet of Complete Mini EDTA-free protease inhibitor (Roche Diagnostics,, Cat #11 836 170 001) per 10mL of buffer and then sonicated for 5 minutes in ice cold water. The lysed cells were then centrifuged at 5000 RPM with a table top microcentrifuge for 5 minutes at 4˚C. The protein concentration was determined using bicinchoninic acid (BCA) method (ThermoFisher Scientific, Cat # 23227) and supernatants stored at -80˚C.

Samples were diluted with lysis and protease inhibitor buffer up to the desired protein concentration, yielding whole cell lysate (50µg) in 20µL and 20µL loading buffer (5% glycerol,

5% β-mercaptoethanol, 3% SDS and 0.05% bromophenol blue). To denature the proteins, the 40µL sample was heated in boiling water for 5 minutes. Sodium dodecyl sulphate-polyacrylamide gel electrophoresis (SDS-PAGE, the separating buffer (370 mM Tris-base (pH 8.8), 3.5 mM SDS), and the stacking buffer (124 mM Tris-base (pH 6.8), 3.5 mM SDS), were placed in running buffer (25 mM Tris-base, 190 mM glycine, 3.5 mM SDS) and samples, along with the Precision Plus Protein^{TM} Standards Dual Color (Bio-Rad, Hercules, CA, Cat#161-0374), were loaded into the Arcylamide gel (12.5 %) for molecular weight determination at 120 V. After electrophoresis, proteins were transferred overnight, at 4˚C and 180mA, in transfer buffer (25mM Tris-base, 192mM Glycine, 20% methanol), onto PVDF (Bio-Rad, Cat#162-0177). Thereafter, membranes were blocked for 1 hour with gentle shaking in a solution of non-fat dry milk (5% w/v) dissolved in TBS-T buffer (10 mM Tris-base (pH 8.0), 150 mM sodium chloride, 0.5% Tween-20). The membranes were then incubated with a rabbit anti-Wave2 or Cx3Cr1 primary antibody (1:500) diluted in blocking solution at room temperature for 1 hour. Any unbound antibody was removed using three washes of 15 mL TBS-T at room temperature. Membranes were incubated on a shaker for 1 hour at room temperature with HRP (horseradish peroxidase) conjugated anti-rabbit (1:2000) secondary antibody and washed again with TBS-T. Finally, Cx3cr1 and Wave2 was visualized by exposure the chemiluminescent substrate (Perkin Elmer, Waltham, MA, cat#.NEL102001EA) for 1 minute and briefly exposed on a Kodak film.

Immunohistochemistry

To fix the tissue, animals sacrificed for immunohistochemistry were perfused with 40mL of 4% PFA (100mL: 4g paraformaldehyde, 100mL 0.1M PBS) in 0.1M PBS (1000mL: 0.2g potassium chloride, 8.0g sodium chloride, 100mL 0.1M phosphate buffer pH 7.4, 900mL distilled water). Brains were then extracted and placed into vials containing 4%

paraformaldehyde and put on ice. 24 hours later brains were transferred to a 10% sucrose solution. 24 hours later brains were transferred into a second 10% sucrose solution. 24 hours later brains were transferred into a 30% sucrose solution. Brains were kept at 4°C throughout the procedure.

Brains were flash frozen using Freeze'It (Fisher Scientific) and sectioned on a cryostat (Thermofisher) at 3 x 20µm 1 x 60µm thickness. 20µm sections were collected in well plates containing 1mL 0.1M PBS with 0.01% azide (1010ml: 10mL 1% sodium azide, 1000mL 0.1M PBS) and stored at 4°C for fluorescent staining. 60µm were collected in the same manner for 3,3'-Diaminobenzidine staining.

For fluorescent microscopy, sections were co-stained with cluster of differentiation 68 (CD68) (rat anti-mouse, Bio-Rad Antibodies, MCA1957), ionized calcium binding adaptor molecule 1 (IBA1) (rabbit anti-mouse, Abcam, and tyrosine hydroxylase (TH) (Immunostar, 22941). CD68 and IBA1 staining measures microglial activation while TH staining measures dopamine levels. Sections were rinsed 3 x 5 minutes with 10 mM PBS and then blocked for 30 minutes using 250µL blocking solution per well plate (50mL: 2500µL normal goat serum (NGS), 1500µL 10% Triton-X, 46mL 10mM PBS). Blocker was extracted and replaced with 200µL of 1° antibodies at 1:2000 antibody to primary dilution solution (50mL: 2500µL NGS, 1500µL Triton-X, 7.5mL 2% bovine serum albumin (BSA), 38.5mL 0.1M PBS) ratio for CD68, IBA1 and TH overnight. Sections were washed 3 x 5 minutes in 0.1M PBS and then placed in 200µL of 1:1000 2° antibody to primary dilution solution ratio for CD68 (Alexa Fluor 488 goat anti-rat IgG, ThermoFisher, A11006) and IBA1 (Alex Fluor 647 goat anti-rabbit IgG, ThermoFisher, A21246), and 1:500 for TH (Alex Fluor 350 goat anti-mouse IgG, ThermoFisher, A11068) for 3 hours. Sections were then washed 3 x 5 minutes in 0.1M PBS, mounted on

microscope slides and coverslipped using fluoromount (Sigma-Aldrich, St. Louis, MO). Sections set flat on paper towel overnight to dry. 24 hours later, nail polish was applied to the edges to seal them. Sections were covered in tin-foil after 2° antibody application to eliminate photobleaching.

DAB staining for TH was performed to quantify the amount of DA cells in the SNc. 60µm sections were rinsed 2 x 5 minutes in 0.1M PBS and then incubated in 0.3% hydrogen peroxide (50mL: 500µL 30% H_2O_2 in 50mL PBS), 500µL per well. Sections were rinsed 3 x 10 minutes in 0.1M PBS and the blocked using blocking solution for 60 minutes, 250µL per well. Blocker was removed and sections were incubated in 1:2000 anti-TH to primary dilution solution ratio, 200µL per well, overnight. Sections were rinsed 3 x 5 minutes in PBS and then incubated in 1:200 anti-mouse horse radish peroxidase (HRP) (Sigma-Aldrich, S5906) to secondary dilution solution (50mL: 800µL NGS, 800µL 10% Triton-X, 7.5mL 2% BSA, 40.9mL 0.1M PBS) ratio, 200µL per well for 6 hours. Sections were then rinsed 3 x 5 minutes in PBS and then a DAB reaction was performed. Sections were incubated in 1mL of DAB solution (10mg DAB in 1mL $dH_{2D}D$ combined with 50mL of TrisHCl: 0.3790g Trizma in 50mL dH_2O) for 5 minutes on the Belly Dancer, 1mL per well. After 5 minutes, 50µL of 2% H_2O_2 was added and placed back on the Belly Dancer for 10 minutes. Sections were rinsed 3 x 5 minutes in 0.1M PBS and then mounted on microscope slides.

For animals in the 2nd study, which had the Very Low dose SNc and Hippocampus groups, all DAB methods were repeated the exact same way, except they were stained for nuclei using the Nissl stain (cresyl violet).

Cell Counts and Densitometry

For DA cell counts, 60µm DAB stained sections of the SNc were counted. As half of the tissue was used for fluorescent imaging, serial coronal sections used for DA cell counts amount to half of the SNc. Unbiased estimates of cell number were obtained using an Axio Imager M2 motorized fluorescent microscope (Zeiss) and QICAM 12-bit color camera (QImaging) attached to a motorized stage and connected to a computer running the Stereoinvestigator Software (MicroBrightfield). Confocal and z-stack images were taken on a Zeiss LSM800 AxioObserverZ1 mot (inverted) fully motorized stage running ZenPro (Zen) software. Light sources for the confocal microscope came from an X-cite 120 mini LED and transmitted LED, as well as 4 loser lines: 405nm, 490nm, 561nm, and 639nm. Contours of the entire SNc were drawn. Cells were counted at 63x magnification, and tissue thickness was manually measured at every grid site (90µm by 90µm, counting frame: 60µm by 60µm, guard height: 3µm, optical dissector height: 15µm). The neuronal cell count reported was the estimated population using number weighted thickness.

Densitometry was performed on the 20µm tissue sections stained for CD68, IBA1, and TH. The same equipment and software used for the DAB cell counts was used for densitometry except an ORCA-R^2 fluorescent camera (Hamamatsu) which replaced the QImaging color camera. Virtual tissue images were generated and ImageJ software (NIH) was used to compare fluorescence intensities.

Statistical Analysis

All analysis was computed using SPSS (IBM). Cell counts and rotarod behavior statistical analysis was performed using a 1-way analysis of variance cell mean model. Micromax data was

analyzed using a 2-way repeated measures ANOVA model. Western blots were analyzed using a 2-way ANOVA model. Tukey's HSD was used as the post-hoc test as all pairwise comparisons were of interest.

Results

Pilot Study

A pilot study was conducted which used a small group (n = 5) of animals to determine which toxin, QD-SAP or Mac-1-SAP, would be most useful as a microglial depletion strategy in the SNc. To this extent, a single dose of either MAC-1-SAP (2μg) or QD-SAP (0.025μM) was infused into the SNc of c57Bl6/n mice. A subset of animals from each toxin group (at least 2 of 5 per group) displayed circling behaviours and met experimental endpoint criteria by day 5 post-surgery. All animals were perfused on experimental day 6 and brains were collected for immunohistochemistry. SNc sections were stained for TH and CD68 (Fig. 1). Immunofluorescent staining highlighted an increase in microglia activation through increases in CD68 staining intensity at both MAC-1-SAP and QD-SAP infusion sites. Staining with CD68 on the ipsilateral side was so strong that it bled through all the other channels (Fig. 2). Therefore, intensity of TH (blue) could not be compared. However, there was a noticeable decrease in intact TH+ cell bodies on the ipsilateral side compared to the control.

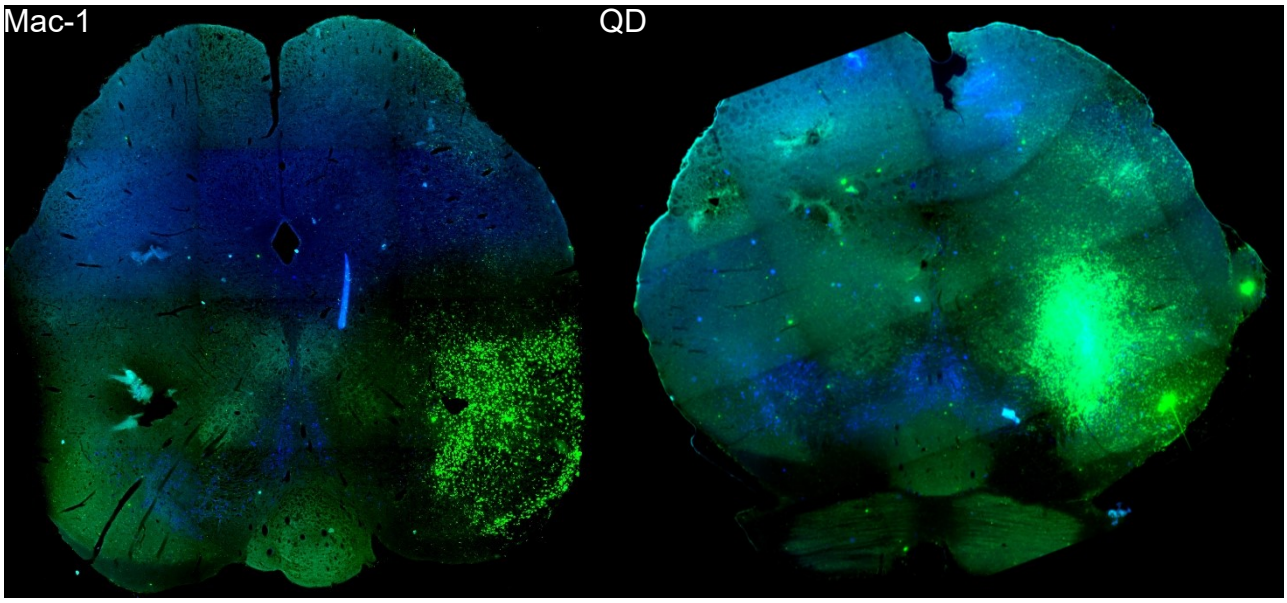

Figure 1. Representative images of pilot tissue showing MAC-1-SAP and QD-SAP mediated microglial activation in the SNc. MAC-1-SAP (2µg) and QD- SAP (0.025µM) site is on the right of each brain slice. Green: CD68. Blue: TH.

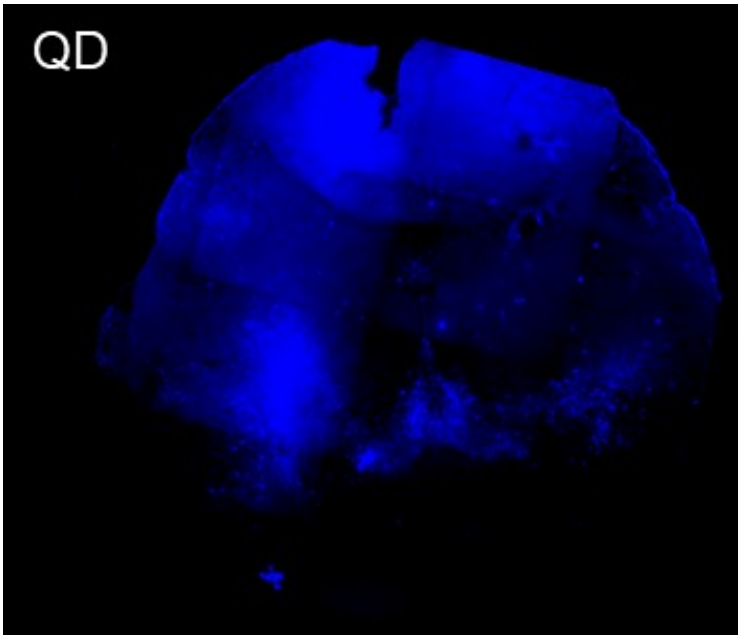

Figure 2. Pilot tissue showing the fluorescent bleed through of CD68 (488nm) into the channel occupied by TH (350nm). Left: Ipsilateral side.

QD-SAP is selectively taken up by microglia causing dopaminergic degeneration in the SNc

QD-SAP was selected as the toxin to be further characterized as a microglia-specific toxin as it showed similar, albeit more robust effects, compared to Mac-1-SAP, but had the added advantages of biostability and autofluoresence (Jaiswal, Mattoussi, Mauro, & Simon, 2003). A follow up study termed QD1 was performed which A: titrated the dose, B: performed more comprehensive histology, C: added behavior and biochemical data, and D: increased the sample size.

As the pilot study reported an increase in IBA1+ staining, which could be indicative of microglial activation, we wanted to confirm microglial specific uptake of QD-SAP. Using high magnification confocal microscopy and z-stack imaging on control animals administered unconjugated QD's, we showed that QD's were only grouped together and colocalized within microglia. A single z-layer (Fig. 3) shows that QD-SAP (C), is colocalized to IBA1+ microglia (B) when merged (D), and not colocalized with TH+ neurons, (A). 3D reconstruction of the z-stack images shows that QD's are only found in clusters when colocalized with IBA1 (video available).

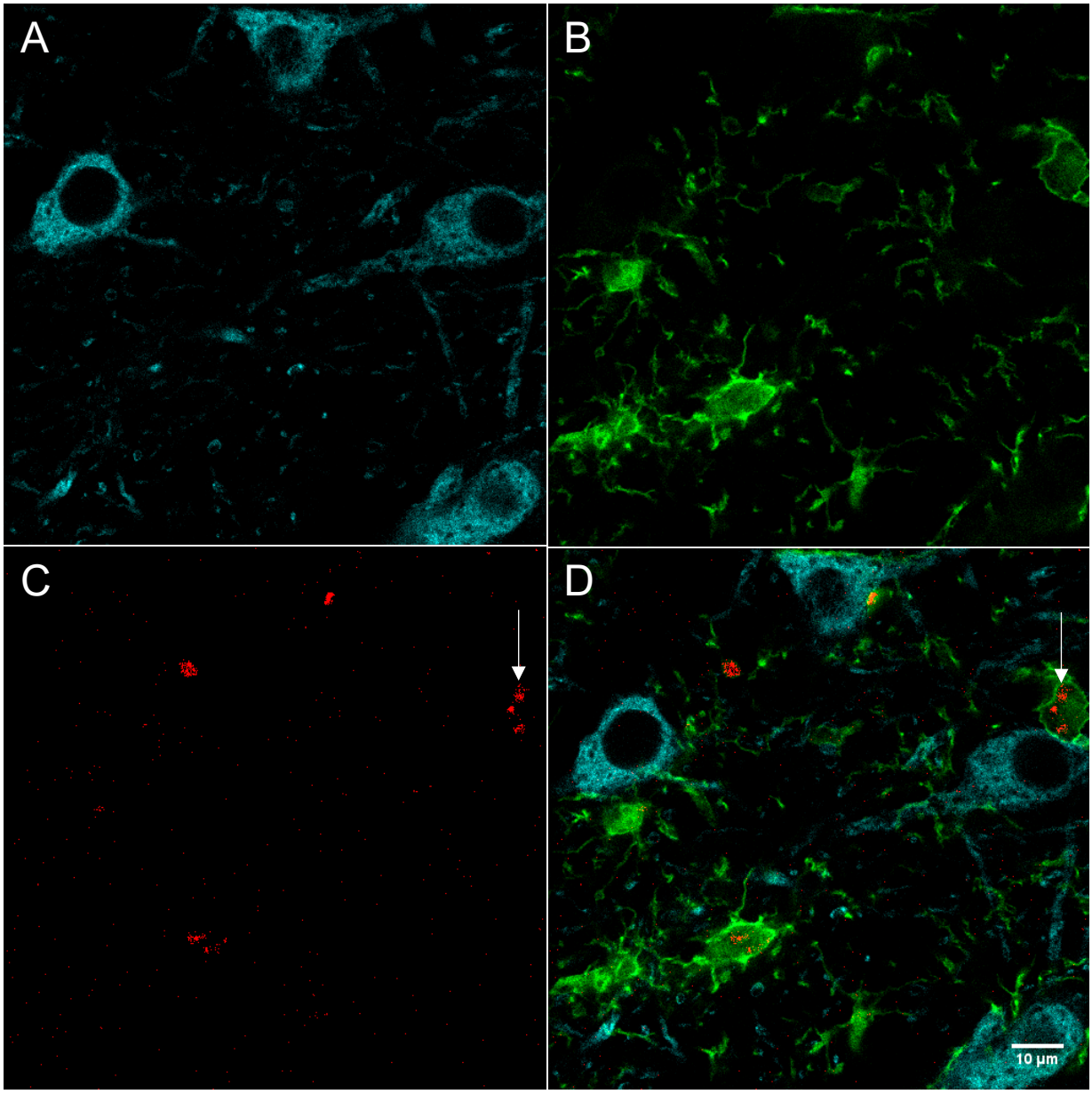

Figure 3. Confirmation microglia-specific uptake of QD's (mutli-panel 63x zoomed in image). Image taken on the ipsilateral side posterior to the injection site of a 7 Day unconjugated QD SNc Control animal. This image is a single layer of a Z-stack which was used to create a 3D reconstruction of the cells in the area. A: TH+ positive neurons, B: IBA1+ microglia, C: unconjugated quantum dots, and D: merge. Arrow tip is directly above a cluster of QD's (C) inside microglia (D)

The other unexpected finding of the pilot was that the TH staining, while shrouded by the bleed through of the CD68 staining, showed less intact TH+ dopaminergic cell bodies on the ipsilateral side of injection compared to the contralateral side. To quantify this phenomenon, we

performed DAB TH+ cell counts in the SNc of saline control, low QD-SAP, and high QD-SAP animals (Fig. 4 and 5). As every second slice of SNc tissue was collected for immunohistochemistry, an entire stereological analysis of the SNc could not be performed. Nonetheless, a representative area of the SNc could be collected using 6 slices centered around the infusion site. We found that administration of QD-SAP caused a significant reduction in overall TH+ dopaminergic neuron cell counts ($F(2,7) = 8.332$, $p < 0.014$) (Fig. 5), with the

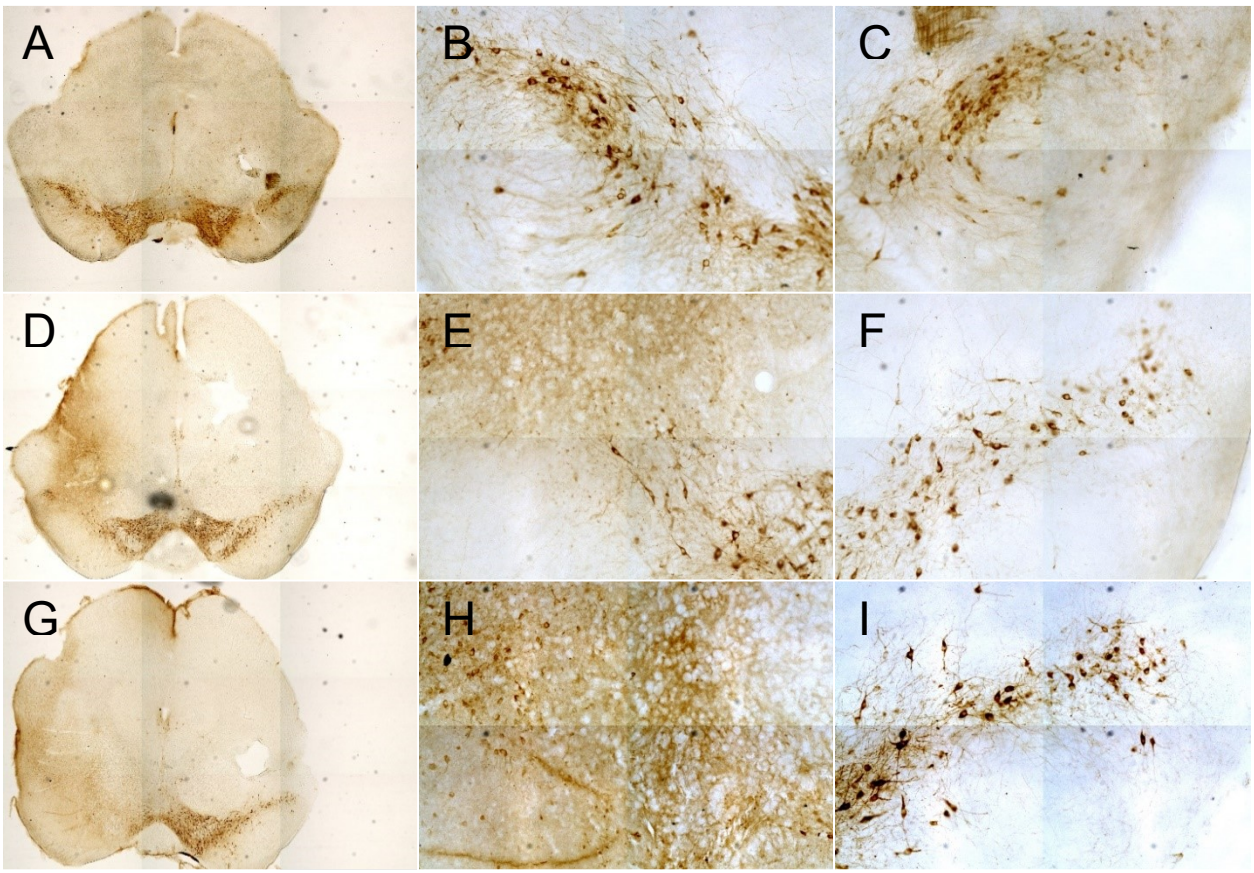

Figure 4. Dose effects of QD-SAP on TH+ dopaminergic cells in the SNc. Virtual tissue images of saline control (A-C), low dose (D-F), and high dose (G-I) of QD-SAP shows that both low and high treatment cause degeneration of dopaminergic neurons on the ipsilateral side. The left column shows full slice virtual tissue images of the different treatment groups at 5x magnification. The middle column shows a virtual tissue image of the ipsilateral size of injection at 40x magnification, and the right shows the contralateral side.

administration of the high dose of 0.025µM QD-SAP (Fig. 3 G-I) causing a significant reduction in TH+ positive cell counts ($M = 37.70$, $SD = 26.51$) compared to surgical controls ($M = 202.00$,

SD = 26.514) (Fig. 3 A-C). There was no statistically significant difference between the low dose (M = 102.667, SD = 30.436) and control or high dose groups.

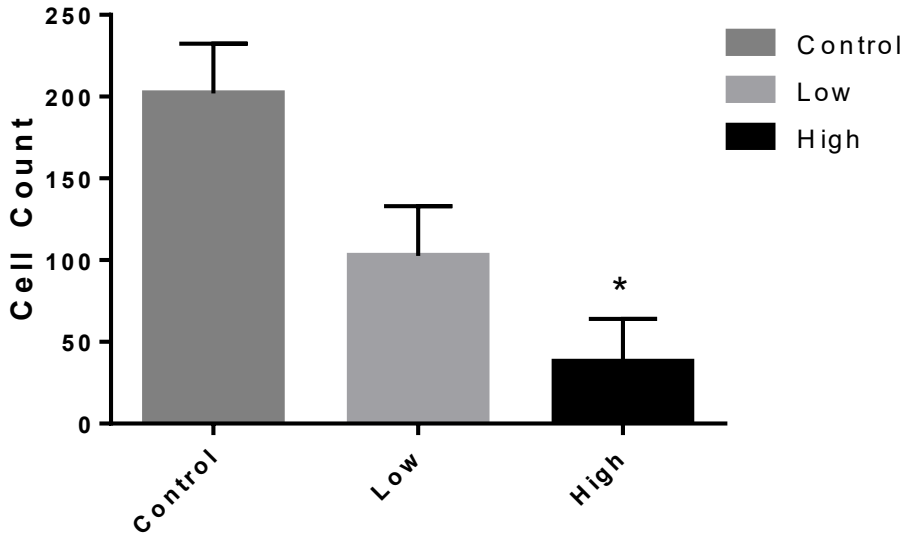

Figure 5. DAB TH+ dopaminergic neuron cell counts in the substantia nigra. Stereological methods were performed using 6 slices of the SNc centered around the injection site. ($F(2,7) = 8.332$, $p < 0.014$)*. Control: Saline.

As follow up on the circling behavior observed in the pilot study, we performed a rotarod behavior test to measure for balance and co-ordination (Fig. 6). A one-way ANOVA for mean latency to fall from the rotarod behavior test reported a significant effect of treatment ($F(2,26) = 6.152$, $p < 0.007$). Post-hoc analysis using Tukey's HSD reported a significant reduction in mean latency to fall when comparing either control (M = 260.933, SD = 64.833) or low dose (M = 238.433, SD = 58.482) treatment groups to the high dose treatment group (M = 149.846, SD = 84.712). There was no significant change in mean latency to fall between control and low dose treatment groups.

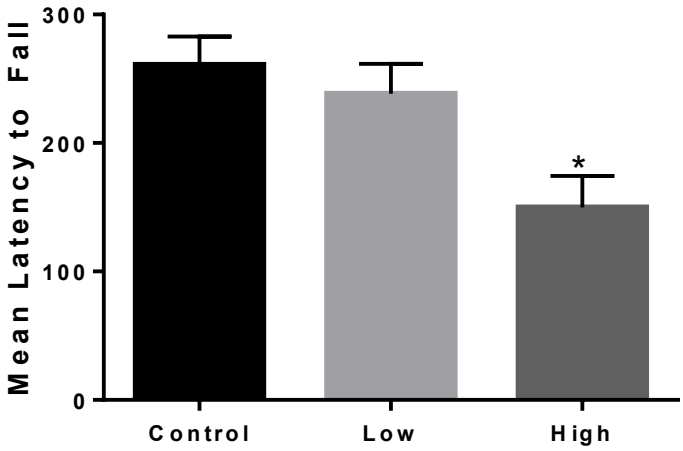

Figure 6. Balance and coordination testing on the rotarod of QD-SAP reports that the high dose had a significant effect on mean latency to fall compared to saline control animals. ($F(2,26) = 6.152$, $p < 0.007$)*.

QD-SAP induced microglia depletion and subsequent dopaminergic denervation

To disseminate temporal effects of QD-SAP, another experiment was conducted that added 1 and 2-day perfusion timepoints in addition to the previous 7 day timepoint. As QD-SAP animals in previous experiments began circling and trending towards endpoint conditions before day 7, it was predetermined in this experiment, all animals in the 7 Day timepoint group would be euthanized early if any of the animals began uncontrollably circling – this did happen on experimental day 4, therefore, 7 Day animals were all perfused 4 days post-surgery. To simplify reporting and discussion, all 7 Day QD2 animals will be referred to as 4 Day animals.

Administration of the high dose of QD-SAP shows a progressive loss of dopaminergic neurons beginning 1 day post-surgery (Fig. 7 C,D), and continuing until endpoint conditions 4 days post-surgery (Fig. 7 G,H). IBA1+ microglia show increased staining intensity in the 7 Day

unconjugated control animal (Fig. 7 B), and decreased staining intensity in the QD-SAP animals of all timepoints (Fig. 7 D,F,H).

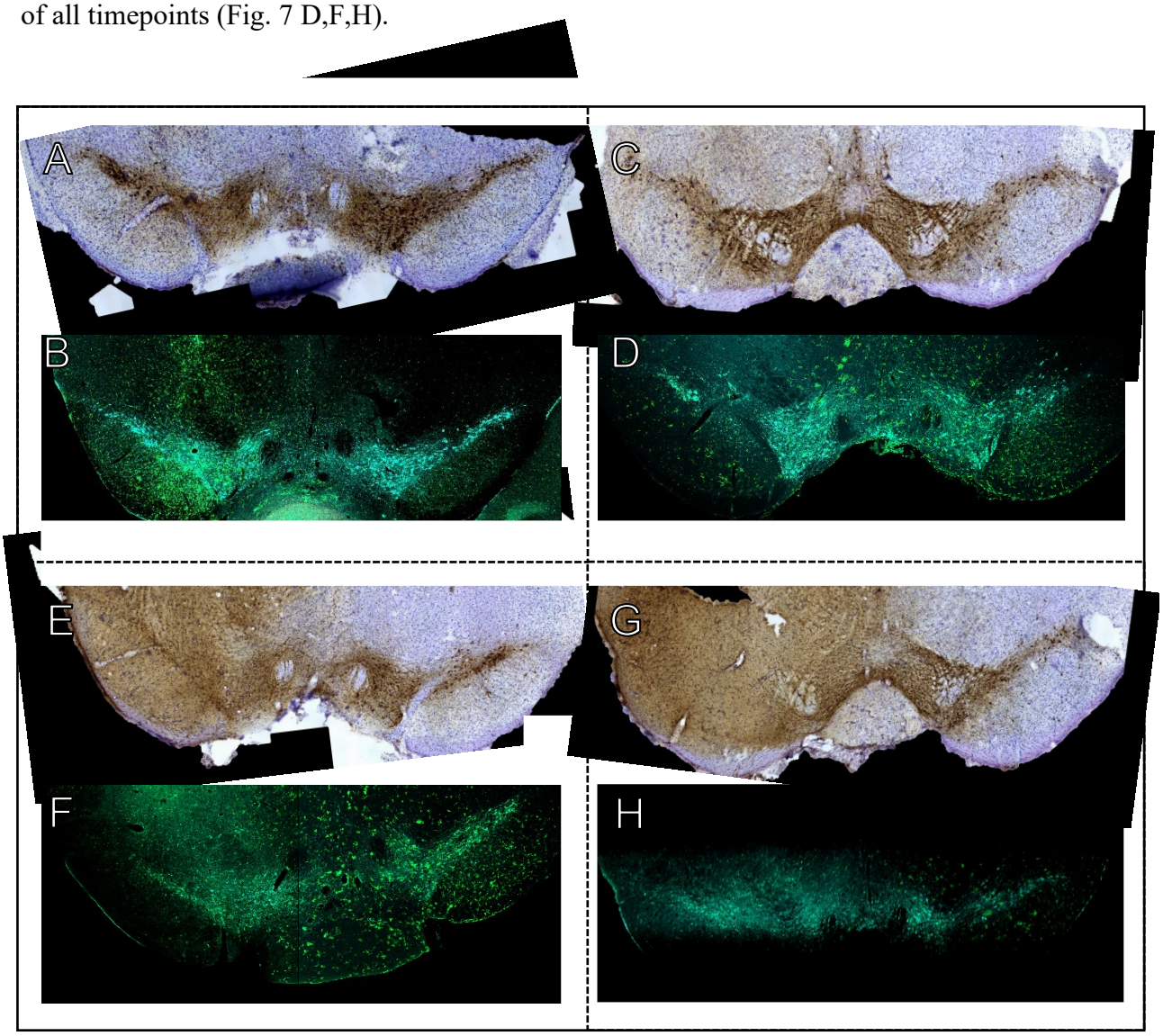

Figure 7. Temporal effects of high dose QD-SAP on IBA1+ microglia and TH+ neurons compared to 7 Day unconjugated-QD controls (A and B). Animals that received QD-SAP showed a depletion of microglia starting 1 day post-surgery (C and D), and a progressive loss of intact dopaminergic neurons continuing into 2 Day (E and F) and 4 day (G and H) timepoints Infusion side: Left, The top virtual tissue slice of each box is aDAB stain for TH+ dopaminergic neurons and a Nissl counterstain for nuclei, while the bottom fluorescent image is an IBA1 stain for microglia (green) and TH (cyan) for dopaminergic neurons.

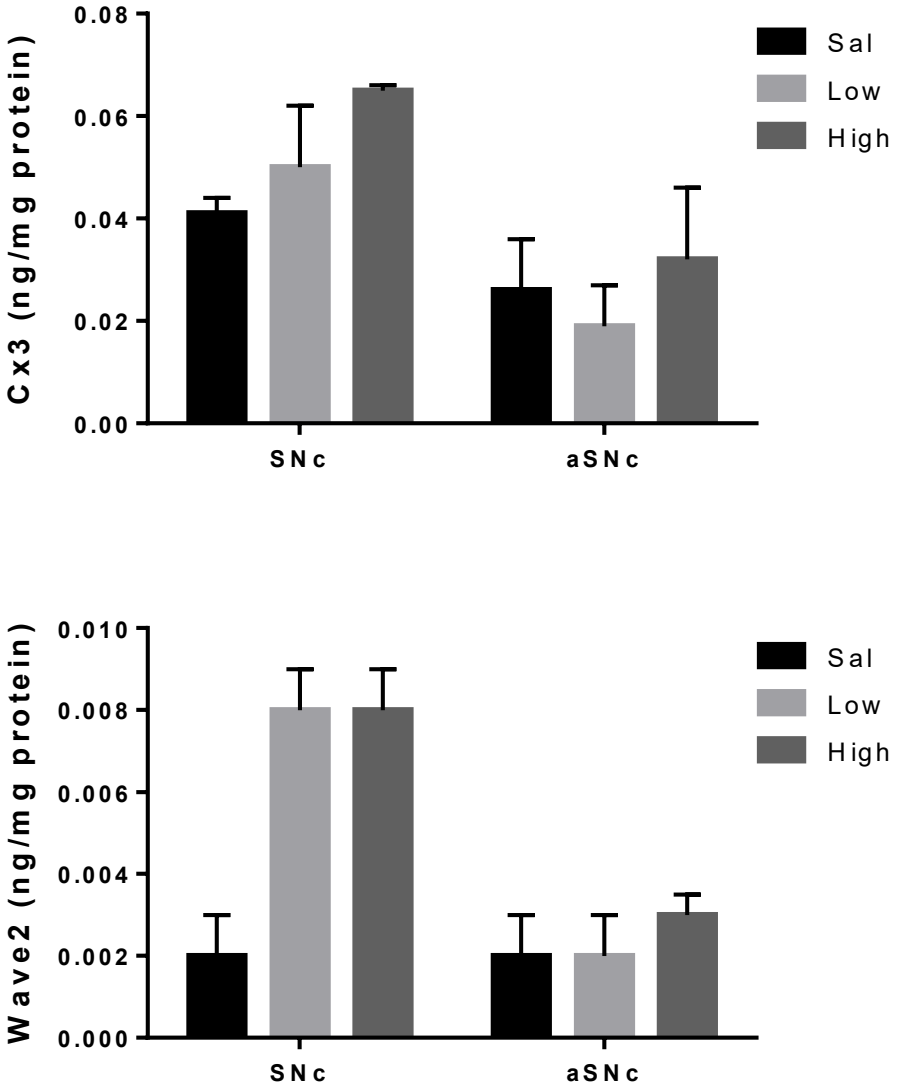

Figure 8. Western blots of pro-inflammatory (Wave2) and anti-inflammatory (Cx3Cr1) markers in the substantia nigra (SNc) and area above the substantia nigra (aSNc). There are no significant effects, but there are trends showing increased pro- and anti-inflammatory signaling within the substantia nigra as QD-SAP dose increases, as well as a trend of increased signaling when comparing the SNc to the area around the SNc. In particular ($F(2,8) = 5.763$, $p = 0.0504$) when comparing Wave2 treatment groups within the SNc. For images see Appendix 1: Western Blot Images.

An initial increase in microglial activation is concurrent with trends in increased cytokine signaling as measured by the anti-inflammatory marker Cx3Cr1 and the pro-inflammatory marker Wave2 (Fig. 8). The sample size for the westerns was low, with an $n = 3$ for each group.

Animals originally designated as rapid decapitation animals for western blots we re-routed for perfusions as some of the animals in the perfusion groups had to be euthanized early. As such, an increased sample size is necessary to adequately comment on the inflammatory profile generated by QD-SAP.

Controls with unconjugated QD's show long term (at least 7 day) activation of microglia post-surgery (Fig. 9). On day 1, there may be a slight difference in microglia cell body size (Fig. 9 IJ) between ipsilateral and contralateral sides (densitometry not yet completed), which by day 7 becomes an obvious difference (Fig. 9 KL). Additionally, the 7 Day control animal IBA1 section (Fig. 9 F) shows that there is a clear increase in microglia activation specifically within the SNc (white box, EF) when compared to the adjacent VTA (red box (EF). No circling behavior effects were seen by animals in any of the control conditions.

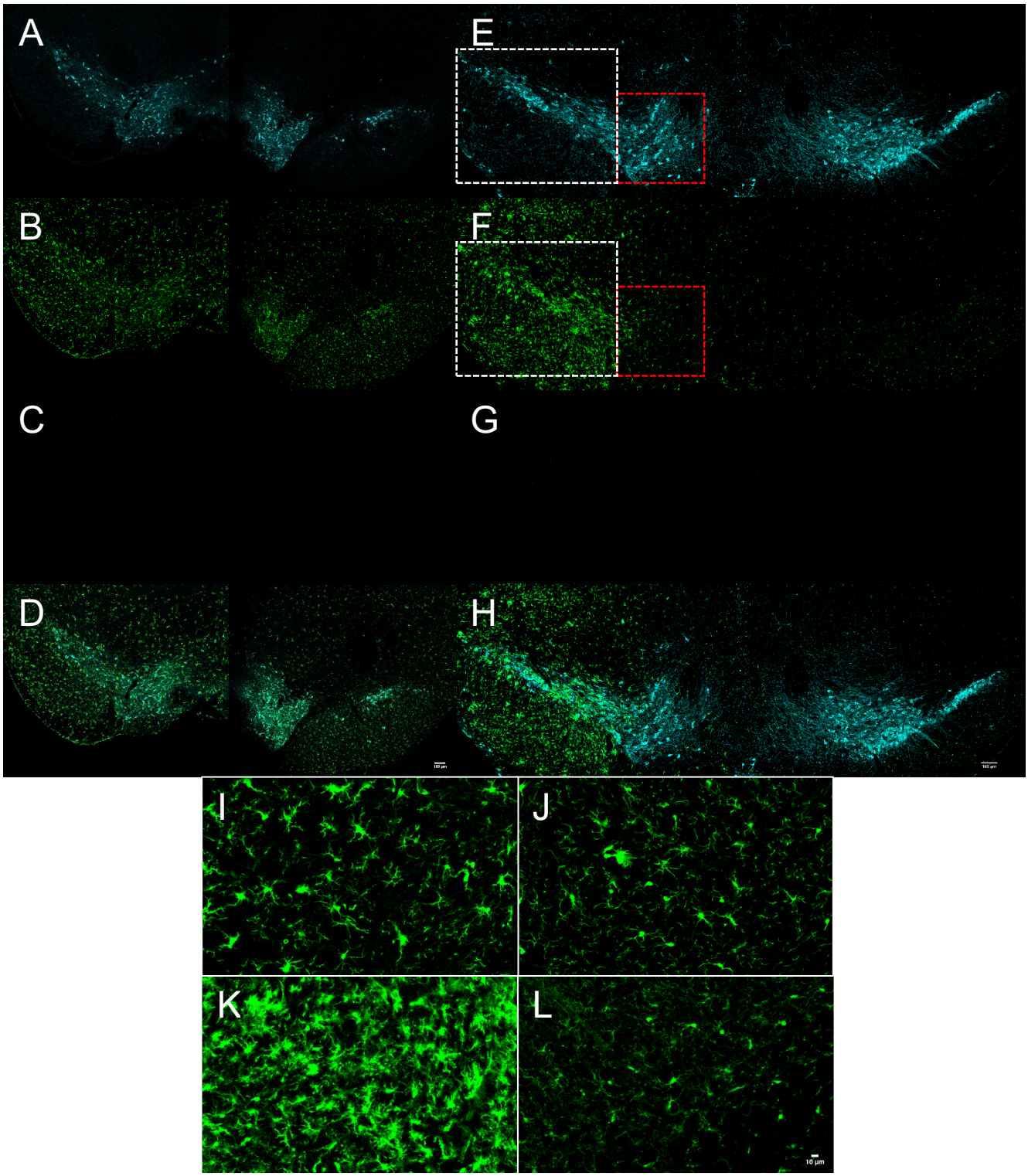

Figure 9. Unconjugated QD 1 (A-D) and 7 (E-H) Day surgical control animals show ipsilateral microglial activation. AE: TH+ positive neurons, BF: IBA1+ microglia, CG: unconjugated quantum dots, and DH: merge. White box: SNc. Red box: VTA. IJ: Zoomed in view of the ipsilateral (I) and contralateral (J) section of 1 Day Control (B). KL: Zoomed in view of the ipsilateral (K) and contralateral (L) of 7 Day Control (F)

Compared to the high dose group, the low dose animals in general showed less uncontrollable

circling behaviors. Therefore, we added another group of SNc QD-SAP animals which was 20% of the original high dose amount. This very low dose amount was the only dose of QD-SAP which showed a 100% survival rate, and behaviorally, compared to all other groups, the very low dose group showed no hyperactivity or uncontrollable circling. They did, however, lose the ability to turn to the right (non-scored video footage available). All animals in this group survived to their experimental endpoint and were perfused for immunohistochemistry. Comparing the ipsilateral (Fig. 10 B-E) to contralateral (Fig. 10 F-I) shows a drastic reduction in TH+ dopaminergic cell bodies coupled with an increase in IBA1+ microglia staining intensity on the ipsilateral side (Fig. 10). The ipsilateral side shows a lesion area around infusion site (above the SNc) which penetrates through all sections both posterior and anterior to the infusion site.

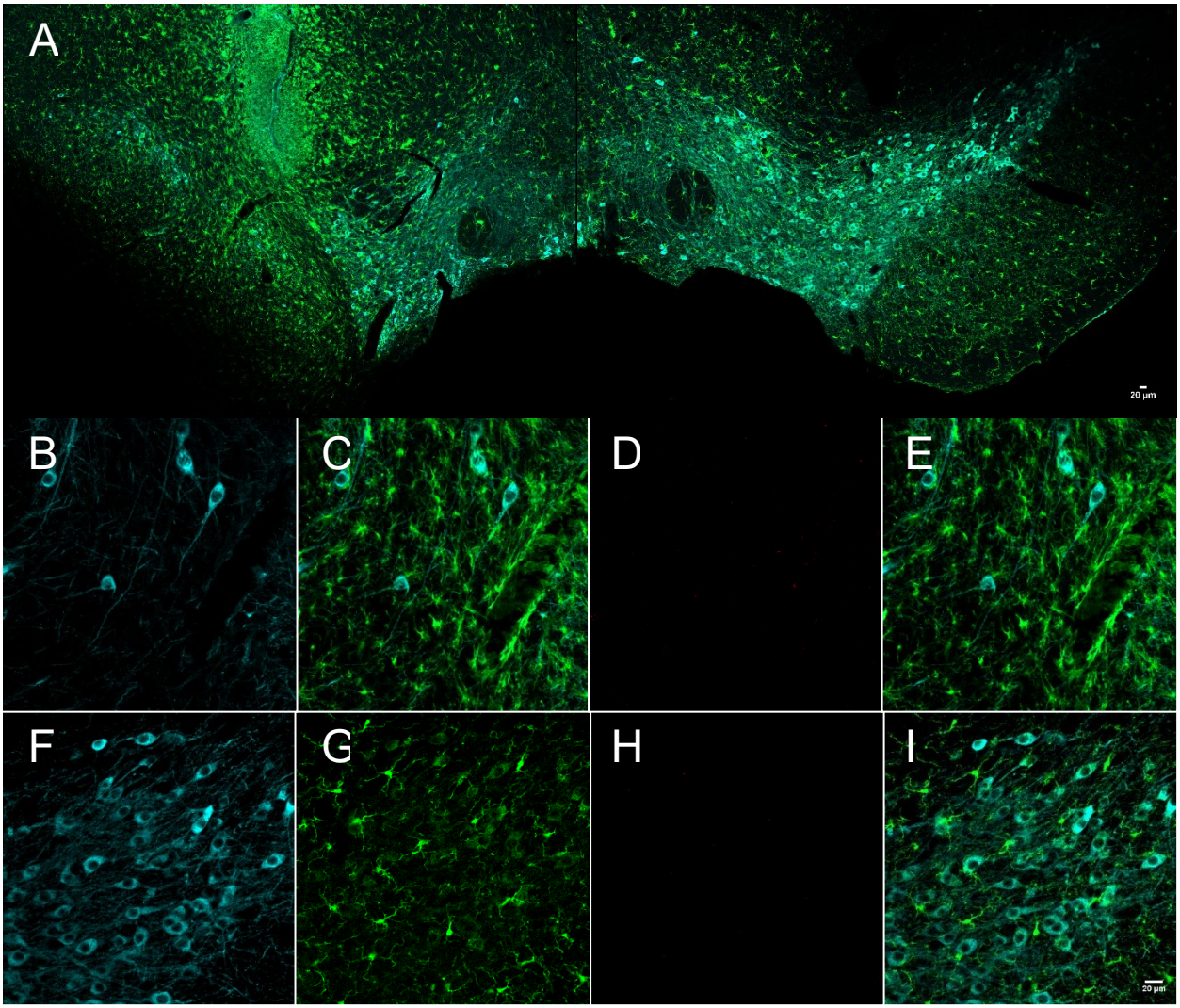

Figure 10. Effects of the Very Low dose of QD-SAP on TH+ neurons and IBA1+ microglia in the SNc. Virtual tissue images show massive damage to neurons and microglial activation on the ipsilateral side on infusion (A). The zoomed in panels on the ipsilateral side (B-E) show a decrease in TH+ neurons (cyan) and increased activation of IBA1+ microglia (green) compared to the corresponding area on the contralateral side (F-I). The channel for QD's on each side (D and H) are faint at 20x magnification, but still show that clusters of microglia are localized to the ipsilateral side.

Administration of QD-SAP shows similar effects in the HPC and SNc

As our experiments within the SNc were showing effects different than our hypothesis, we decided to add a group that would receive an infusion into the hippocampus. So far, the only research performed using QD-SAP was done in the hippocampus, and thus was the main source of information leading into the studies (Minami et al., 2012). Although the high dose (0.025mM)

of QD-SAP was having negative effects in the SNc, we kept that dose the same so that it could be compared to this other study done by Minami and colleagues. Like the SNc infusion groups, the high dose of QD-SAP caused a subset of HPC animals to uncontrollably circle starting 3 days post-surgery, and by day 4, all animals in the group had met endpoints requiring humane euthanasia.

Fig. 12 shows that the high dose of QD-SAP was effective at reducing the number of IBA1+ microglia on the ipsilateral side of injection (Fig. 12 B) compared to the HPC control (Fig. 12 A). As we saw the same circling behavior in HPC animals that received the toxin, we decided to stain SNc tissue in HPC animals and *vice versa*. Interestingly, HPC animals showed a large loss of intact TH+ dopamine neurons in the SNc (Fig. 13 A) compared to HPC controls (Fig. 13 B), which seemed to penetrate throughout the SNc (Fig. 13 C-E). The reverse effect where animals injected with QD-SAP caused destruction of neurons in the HPC was not seen (Fig. 12 A-D).

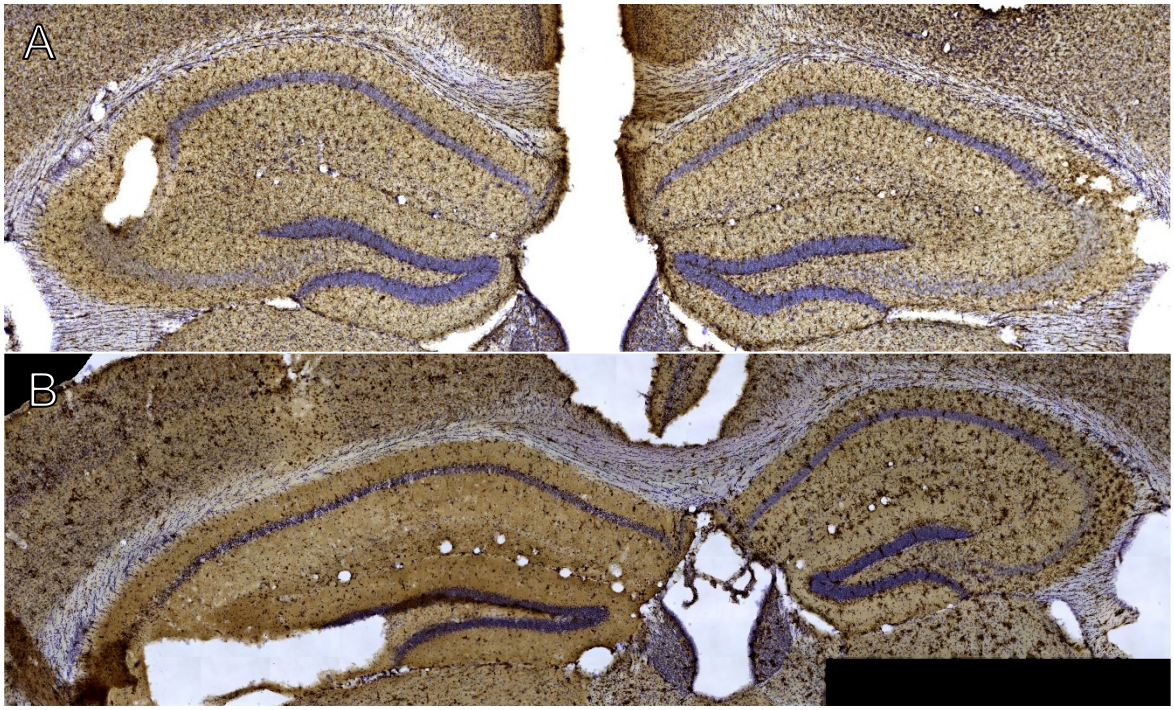

Figure 12. QD-SAP HPC animals show near complete ablation of microglia on the ipsilateral side of injection, with potential neuronal damage (B), while HPC controls show no signs of microglial depletion or neuronal damage (A). The left side of each virtual tissue slice is ipsilateral to the infusion site. Stain: DAB IBA1+ microglia with a Nissl counterstain.

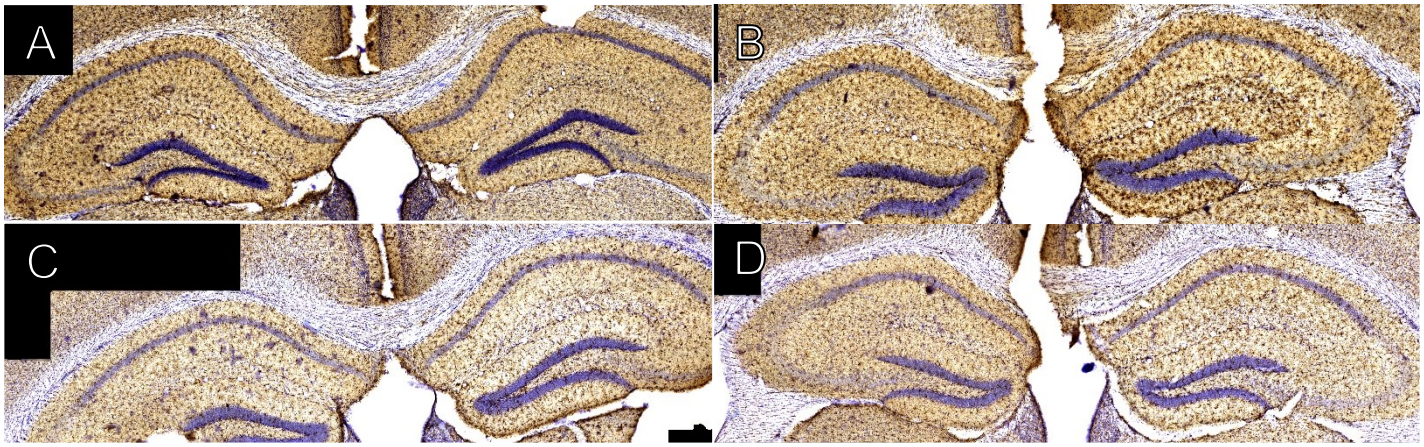

Figure 11. 2 day SNc Control (A) and SAP (B), 7 Day SNc SAP (C), and 1 Day SNc SAP (F) all show no signs of microglial depletion or neuronal damage. The left side of each virtual tissue slice is ipsilateral to the infusion site. Stain: DAB IBA1+ microglia with a Nissl counterstain.

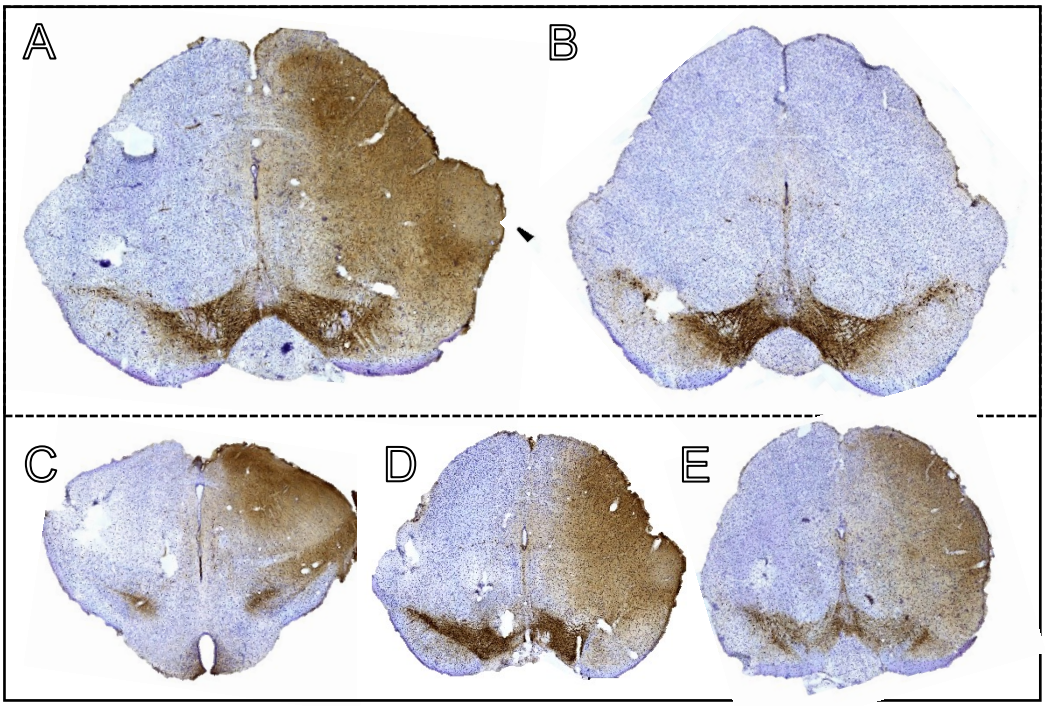

Figure 13. HPC QD-SAP animals show dopaminergic denervation in the substantia nigra (A), while HPC control animals have intact neurons throughout (B). QD-SAP in the HPC This penetrates throughout the SNc (C, D and E). The right side of each virtual tissue slice is ipsilateral to the infusion site. Stain: DAB IBA1+ microglia with a Nissl counterstain.

Neurons in the QD-SAP HPC animals shown by a Nissl counterstain (Fig. 12 B) appeared to be more damaged than HPC control animals (Fig. 12 A). Immunofluorescence of the same animal in Fig. 12 shows that QD-SAP is indeed causing depletion of microglia and neuronal death in the ipsilateral side of QD-SAP injection (Fig. 14 A). Additionally, 4-day QD-SAP SNc high dose animals do not appear to cause any damage to HPC neurons (Fig. 14 B).

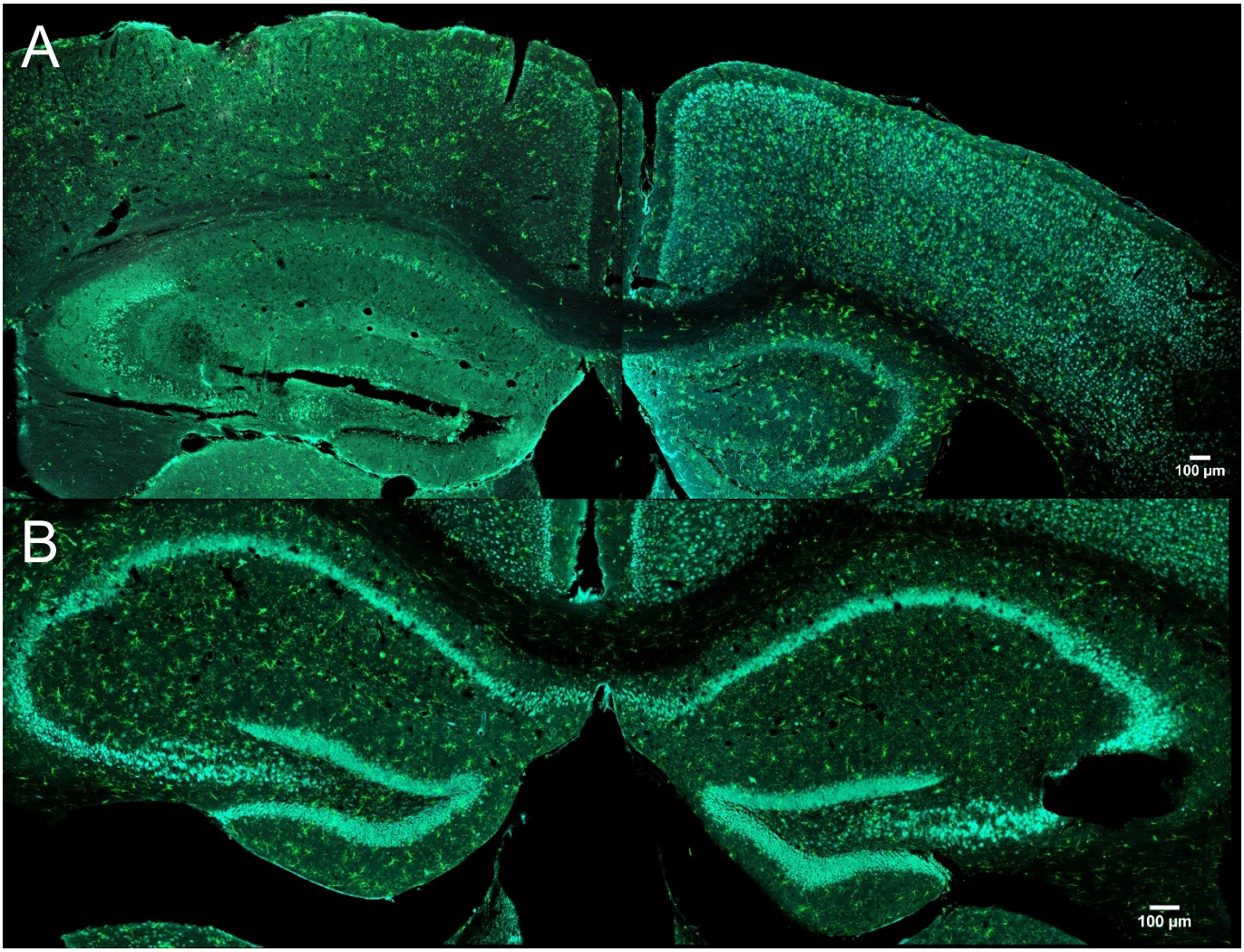

Figure 14. QD-SAP HPC animals show heavy neuronal damage on the ipsilateral side of injection (A), while 4 Day SNc QD-SAP animals show no effects to neurons on the ipsilateral side (B). The left side of each virtual tissue slice is ipsilateral to the infusion site. Stain: IBA1+ microglia (green) and Neun (cyan).

Discussion

The initial goal of this investigation was to assess the use of targeted saporin treatment as a microglia depletion system for use in PD research. Our pilot study used two independent microglia targeting strategies—quantum dots and MAC-1—to evaluate the efficacy of each microglia targeting strategy, and to determine the most effective system. Fluorescent staining in the pilot study, coupled with the circling behavior of the animals injected with either QD-SAP or MAC-1-SAP suggested that a robust inflammatory response and dopaminergic cell death was induced by these treatments. Although both treatments elicited similar outcomes, the QD-SAP treatment had the added advantage of auto-fluorescence and biostability. Hence, QD-SAP was chosen as the toxin to explore in further detail and two subsequent experiments were aimed at characterizing the cellular, biochemical, behavioral, dosage, and regional effects of QD-SAP.

QD-SAP causes depletion of microglia and dopaminergic neurons in the SNc

IBA1 immunofluorescent imaging of 1, 2 and 4-day SNc QD-SAP treated animals revealed a clear depletion of microglia at the infusion site compared to controls (Fig. 7) This was contrary to what we observed in our pilot study, where increases in CD68 staining led us to believe that microglia were not being depleted but being activated. We think the fact that CD68 is found within lysosomal membranes and does not highlight microglial processes resulted in us missing the possibility that the CD68 antibody was binding to extracellular debris from dying microglia (Holness & Simmons, 1993). We do not have data showing a time course increase in inflammatory factors; however, previous work has shown peak brain inflammatory responses within 1 hour of insult, and we have found increased protein levels of a proinflammatory marker, Wave2 (Fig. 8). Thus, we suggest that microglia first undergo marked inflammatory processes before eventually dying (Qin et al., 2007).

Following depletion of microglia, there was a dramatic and progressive decrease in dopamine neuronal survival in the SNc. Indeed, dopamine neuron counts confirmed that targeted infusion of QD-SAP caused a clear decrease in the number of TH+ soma compared to controls (Fig. 4 and 5). To confirm that QDs were not being taken up into neurons and directly killing the cells, 3D reconstruction of confocal z-stack images was used to show that unconjugated QD's were in fact, found exclusively in microglia (Fig. 3).

The fact that dopaminergic neurons in the SNc degenerate following disruption of homeostatic microglial mechanisms is not surprising. Indeed, numerous PD models involve microglial priming towards an inflammatory state, resulting in the progressive loss of SNc DA neurons. For example, priming of microglia by a non-toxic dose of LPS significantly increases dopaminergic cell loss in the 6-hydroxydopamine and paraquat model of PD (Koprich, Reske-Nielsen, Mithal, & Isacson, 2008; Mangano and Hayley, 2009); upregulation of microglial NADPH activity is pivotal in the rotenone model of PD (Gao, Hong, Zhang, & Liu, 2002) and blockade of microglial activation protects DA neurons in the MPTP model of PD (Wu et al., 2002).

What is unknown is the relative contributions that the initial activation and the subsequent depletion of microglia have on SNc dopaminergic degeneration. It is known that neuronal degeneration *in vivo* models of PD can be rescued by blocking microglial activation, suggesting that the initial microglial activation may be the cause of the degeneration (Schober, 2004; Wu et al., 2002). There has also been *in vitro* work that reports that a lack of microglia is protective against toxins used to destroy dopaminergic cells (Gao et al., 2002). We propose that the contributions are temporally dependent, where an initial increase in inflammation followed by a subsequent decrease in homeostatic mechanisms causes dopaminergic neurons to

degenerate rapidly. Nonetheless, we do not have enough definitive evidence to confirm this hypothesis. Subsequent experiments are required that target the depletion of microglia in the SNc without eliciting an inflammatory response, and so far, ours is the only study which has collected *in vivo* results of the effect of microglial depletion on dopaminergic neurons.

QD-SAP as a tool to destroy neurons in the SNc

The initial goal to use targeted saporin treatment to selectively destroy microglia in the SNc will obviously not come to fruition, as dopaminergic neurons did not survive the treatment. Using two doses of QD-SAP (0.025mM, 0.015mM respectively), we repeatedly saw the same outcome: a subset of animals in each group would being to show signs of circling behavior 3 days post-surgery. Animals in the high dose group would begin to show severe circling and sickness behaviors by day 4, and by day 6, most animals would have to be humanely euthanized. These doses of QD-SAP are therefore not useful tools in destroying SNc neurons. However, another group of animals received a very low dose of QD-SAP (0.005mM). These animals showed no adverse effects from the treatment and reached their experimental endpoint 7 days post-surgery. Interestingly, all animals in this very low dose group were unable to turn to the right, and the preliminary data shows the same loss of dopaminergic neurons in the SNc as the other doses (Fig. 10). Thus, the sickness effects of the toxicant appear to be more sensitive to dose than the dopaminergic neurotoxicity.

Regional Effects of QD-SAP

As our initial experiments in the SNc reported different findings than Minami and colleagues (2012b), who were the only lab to have published QD-SAP research and this involved hippocampal (HPC) infusions, we attempted to replicate and expand on their work. They

reported that, in HPC slice cultures, QD-SAP completely ablated microglia and protected neurons from amyloid-β induced neuronal loss. Similarly, *in vivo* they reported that unconjugated QD's stayed within hippocampal microglia for up to 28 days without any adverse effects (Minami et al., 2012). We added an *in vivo* HPC group to elaborate on their findings, and our preliminary results indicate that QD-SAP works *in vivo* in a different way than *in vitro*. Our findings agree with their report that unconjugated QD's enter microglia in the HPC without affecting neurons, and expand on their findings by showing that QD-SAP animals exhibit the exact same microglial depletion and neuronal loss as SNc animals (Fig. 14).

To our surprise, however, the HPC group in our study showed the same circling behaviors as our low and high dose SNc animals, and astonishingly, we found that animals given an injection of QD-SAP into the hippocampus exhibited the exact same dopaminergic degeneration in the SNc (Fig. 13). We hypothesize that a wave of microglial activation spreads from the HPC far enough to reach the SNc where the activated microglia then cause the destruction of DA neurons. Indeed, our preliminary data consistently shows that HPC animals have neurodegeneration in the SNc, but conversely, mice with QD-SAP infused into the SNc do not show neurodegeneration in the HPC (Fig. 14).

The region-specific susceptibility of dopaminergic neurons has been previously noted. The SNc compared to the HPC or cortex is significantly more sensitive to challenge by bacterial endotoxin lipopolysaccharide (Kim et al., 2000). SNc dopaminergic neurons also have increased energy demands, making them more vulnerable to oxidative stress (Pissadaki & Bolam, 2013), and increased Ca^{2+} levels due to the reliance on L-type Ca^{2+} channels for their pacemaking activity makes SNc dopaminergic neurons more susceptible than other dopaminergic neurons (Chan et al., 2007).

Together, these findings support our contention that a combination of a QD-SAP induced initial, robust, activation of microglia followed by a subsequent depletion of microglia causes SNc dopamine neurons to degenerate. Intriguingly, since an apparent inflammatory cascade originating in the HPC affected the distant SNc neurons (much like a local injected did), this must be massively robust pathological process. Indeed, our data suggests that animals given QD-SAP in the HPC show the same amount of neuronal loss in as a targeted infusion of LPS into the SNc followed by numerous peripheral infusions of paraquat (Mangano & Hayley, 2009). Additionally, the fact that the SNc neurons degenerated when QD-SAP is administered to the hippocampus, but not vice versa, points to the fact that SNc neurons are far more susceptible, than HPC neurons.

Conclusion

These results shed light on how *in vivo* microglial depletion in the SNc is not a simple process and that any perturbation in microglial homeostasis can have profound consequences for neurons. To the best of our knowledge, QD-SAP is the first agent which, when administered to the HPC, causes SNc dopaminergic cell death. Use of QD-SAP in the HPC in future experiments could help researchers understand the mechanisms of inflammatory propagation in the brain, expand on previous knowledge of SNc dopaminergic neuron susceptibility, and potentially even help characterize different subpopulations of microglia within the brain. Use of QD-SAP at nanomolar doses in the SNc may also provide a novel and robust animal model for PD and related pathologies.

Appendix 1 – Western Blot Image

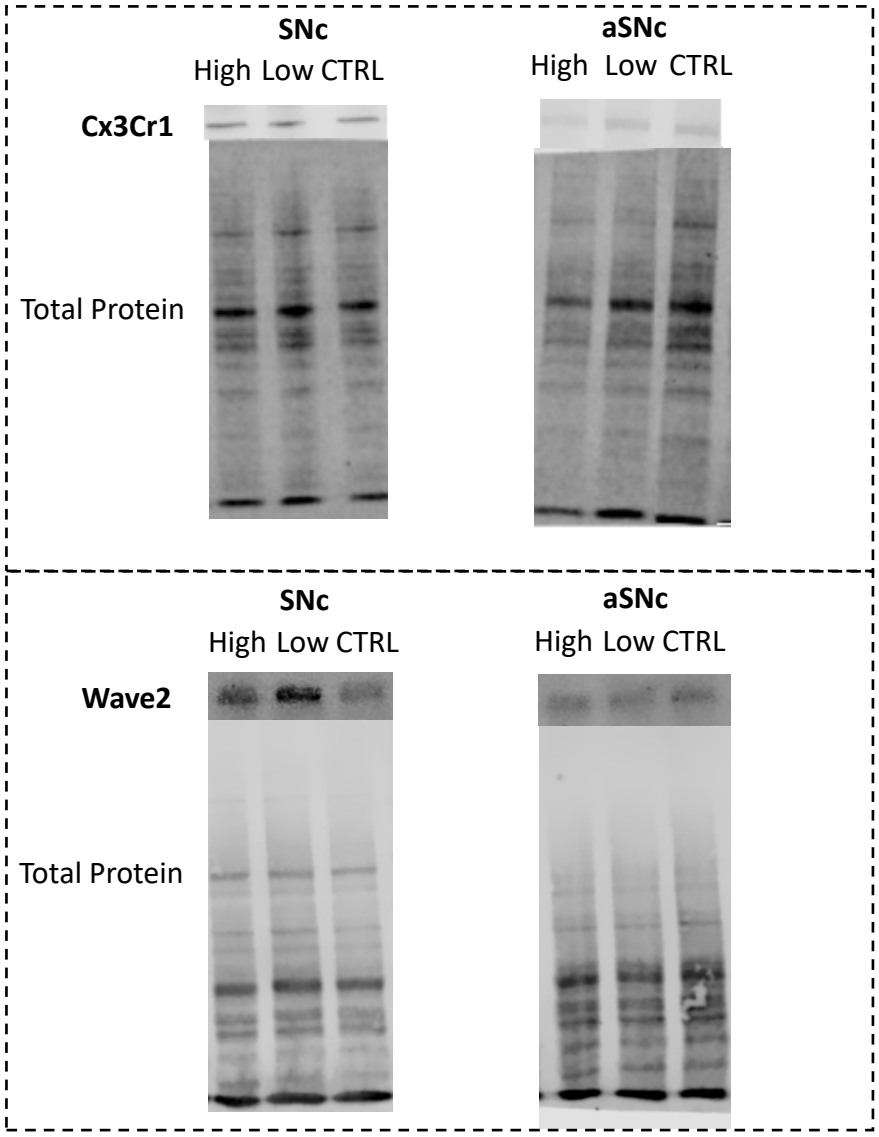

Figure 15. Western Images to corroborate with the data presented in the bar graphs of figure 8.

References

Bagga, S., Hosur, M. V., & Batra, J. K. (2003). Cytotoxicity of ribosome-inactivating protein saporin is not mediated through α2-macroglobulin receptor. *FEBS Letters*, *541*(1–3), 16–20. https://doi.org/10.1016/S0014-5793(03)00280-1

Bagga, S., Seth, D., & Batra, J. K. (2003). The Cytotoxic Activity of Ribosome-inactivating Protein Saporin-6 Is Attributed to Its rRNA N-Glycosidase and Internucleosomal DNA Fragmentation Activities. *Journal of Biological Chemistry*, *278*(7), 4813–4820. https://doi.org/10.1074/jbc.M207389200

Ballou, B., Lagerholm, B. C., Ernst, L. A., Bruchez, M. P., & Waggoner, A. S. (2004). Noninvasive imaging of quantum dots in mice. *Bioconjugate Chemistry*, *15*(1), 79–86. https://doi.org/10.1021/bc034153y

Béraud, D., Hathaway, H. A., Trecki, J., Chasovskikh, S., Johnson, D. A., Johnson, J. A., … Maguire-Zeiss, K. A. (2013). Microglial Activation and Antioxidant Responses Induced by the Parkinson's Disease Protein α-Synuclein. *Journal of Neuroimmune Pharmacology*, *8*(1), 94–117. https://doi.org/10.1007/s11481-012-9401-0

Blakey, D. C., Skilleter, D. N., Price, R. J., Watson, G. J., Hart, L. I., Newell, D. R., & Thorpe, P. E. (1988). Comparison of the pharmacokinetics and hepatotoxic effects of saporin and ricin A-chain immunotoxins on murine liver parenchymal cells. *Cancer Research*, *48*(24 Pt 1), 7072–7078.

Block, M. L., Zecca, L., & Hong, J.-S. (2007). Microglia-mediated neurotoxicity: uncovering the molecular mechanisms. *Nature Reviews Neuroscience*, *8*(1), 57–69. https://doi.org/10.1038/nrn2038

Boscia, F., Esposito, C. L., Crisci, A. D., Franciscis, V. de, Annunziato, L., & Cerchia, L. (2009). GDNF Selectively Induces Microglial Activation and Neuronal Survival in CA1/CA3

Hippocampal Regions Exposed to NMDA Insult through Ret/ERK Signalling. *PLOS ONE*, *4*(8), e6486. https://doi.org/10.1371/journal.pone.0006486

Bruttger, J., Karram, K., Wörtge, S., Regen, T., Marini, F., Hoppmann, N., … Waisman, A. (2015). Genetic Cell Ablation Reveals Clusters of Local Self-Renewing Microglia in the Mammalian Central Nervous System. *Immunity*, *43*(1), 92–106. https://doi.org/10.1016/j.immuni.2015.06.012

Buch, T., Heppner, F. L., Tertilt, C., Heinen, T. J. A. J., Kremer, M., Wunderlich, F. T., … Waisman, A. (2005). A Cre-inducible diphtheria toxin receptor mediates cell lineage ablation after toxin administration. *Nature Methods*, *2*(6), 419–426. https://doi.org/10.1038/nmeth762

Butovsky, O., Jedrychowski, M. P., Moore, C. S., Cialic, R., Lanser, A. J., Gabriely, G., … Weiner, H. L. (2014). Identification of a unique TGF-β-dependent molecular and functional signature in microglia. *Nature Neuroscience*, *17*(1), 131–143. https://doi.org/10.1038/nn.3599

Chan, C. S., Guzman, J. N., Ilijic, E., Mercer, J. N., Rick, C., Tkatch, T., … Surmeier, D. J. (2007). “Rejuvenation” protects neurons in mouse models of Parkinson’s disease. *Nature*, *447*(7148), 1081–1086. https://doi.org/10.1038/nature05865

Chen, Z., Jalabi, W., Hu, W., Park, H.-J., Gale, J. T., Kidd, G. J., … Trapp, B. D. (2014). Microglial displacement of inhibitory synapses provides neuroprotection in the adult brain. *Nature Communications*, *5*, 4486. https://doi.org/10.1038/ncomms5486

Chu, Y., & Kordower, J. H. (2015). The Prion Hypothesis of Parkinson’s Disease. *Current Neurology and Neuroscience Reports*, *15*(5), 28. https://doi.org/10.1007/s11910-015-0549-x

Clausen, B. H., Lambertsen, K. L., Babcock, A. A., Holm, T. H., Dagnaes-Hansen, F., & Finsen, B. (2008). Interleukin-1beta and tumor necrosis factor-alpha are expressed by different subsets of microglia and macrophages after ischemic stroke in mice. *Journal of Neuroinflammation*, *5*, 46. https://doi.org/10.1186/1742-2094-5-46

Couch, Y., Alvarez-Erviti, L., Sibson, N. R., Wood, M. J., & Anthony, D. C. (2011). The acute inflammatory response to intranigral α-synuclein differs significantly from intranigral lipopolysaccharide and is exacerbated by peripheral inflammation. *Journal of Neuroinflammation*, *8*, 166. https://doi.org/10.1186/1742-2094-8-166

Cummings, J. L. (1988). Intellectual impairment in Parkinson's disease: clinical, pathologic, and biochemical correlates. *Journal of Geriatric Psychiatry and Neurology*, *1*(1), 24–36.

Davalos, D., Grutzendler, J., Yang, G., Kim, J. V., Zuo, Y., Jung, S., … Gan, W.-B. (2005). ATP mediates rapid microglial response to local brain injury in vivo. *Nature Neuroscience*, *8*(6), 752–758. https://doi.org/10.1038/nn1472

Dommergues, M.-A., Plaisant, F., Verney, C., & Gressens, P. (2003). Early microglial activation following neonatal excitotoxic brain damage in mice: a potential target for neuroprotection. *Neuroscience*, *121*(3), 619–628. https://doi.org/10.1016/S0306-4522(03)00558-X

Elmore, M. R. P., Lee, R. J., West, B. L., & Green, K. N. (2015). Characterizing Newly Repopulated Microglia in the Adult Mouse: Impacts on Animal Behavior, Cell Morphology, and Neuroinflammation. *PLOS ONE*, *10*(4), e0122912. https://doi.org/10.1371/journal.pone.0122912

Elmore, M. R. P., Najafi, A. R., Koike, M. A., Dagher, N. N., Spangenberg, E. E., Rice, R. A., … Green, K. N. (2014). Colony-Stimulating Factor 1 Receptor Signaling Is Necessary for

Microglia Viability, Unmasking a Microglia Progenitor Cell in the Adult Brain. *Neuron*, *82*(2), 380–397. https://doi.org/10.1016/j.neuron.2014.02.040

Erny, D., Hrabě de Angelis, A. L., Jaitin, D., Wieghofer, P., Staszewski, O., David, E., … Prinz, M. (2015). Host microbiota constantly control maturation and function of microglia in the CNS. *Nature Neuroscience*, *18*(7), 965–977. https://doi.org/10.1038/nn.4030

Galvin, J. E., Lee, V. M., & Trojanowski, J. Q. (2001). Synucleinopathies: clinical and pathological implications. *Archives of Neurology*, *58*(2), 186–190.

Galvin, James E. (2006). Interaction of alpha-synuclein and dopamine metabolites in the pathogenesis of Parkinson's disease: a case for the selective vulnerability of the substantia nigra. *Acta Neuropathologica*, *112*(2), 115–126. https://doi.org/10.1007/s00401-006-0096-2

Gao, H.-M., & Hong, J.-S. (2008). Why neurodegenerative diseases are progressive: uncontrolled inflammation drives disease progression. *Trends in Immunology*, *29*(8), 357–365. https://doi.org/10.1016/j.it.2008.05.002

Gao, H.-M., Hong, J.-S., Zhang, W., & Liu, B. (2002). Distinct role for microglia in rotenone-induced degeneration of dopaminergic neurons. *Journal of Neuroscience*, *22*(3), 782–790.

Gehrmann, J., Matsumoto, Y., & Kreutzberg, G. W. (1995). Microglia: Intrinsic immuneffector cell of the brain. *Brain Research Reviews*, *20*(3), 269–287. https://doi.org/10.1016/0165-0173(94)00015-H

Gilabert-Oriol, R., Weng, A., von Mallinckrodt, B., F. Melzig, M., Fuchs, H., & Thakur, M. (2014). Immunotoxins Constructed with Ribosome-Inactivating Proteins and their

Enhancers: A Lethal Cocktail with Tumor Specific Efficacy. *Current Pharmaceutical Design*, *20*(42), 6584–6643.

Ginhoux, F., Greter, M., Leboeuf, M., Nandi, S., See, P., Gokhan, S., … Merad, M. (2010). Fate Mapping Analysis Reveals That Adult Microglia Derive from Primitive Macrophages. *Science*, *330*(6005), 841–845. https://doi.org/10.1126/science.1194637

Goldmann, T., Wieghofer, P., Müller, P. F., Wolf, Y., Varol, D., Yona, S., … Prinz, M. (2013). A new type of microglia gene targeting shows TAK1 to be pivotal in CNS autoimmune inflammation. *Nature Neuroscience*, *16*(11), 1618–1626. https://doi.org/10.1038/nn.3531

Grathwohl, S. A., Kälin, R. E., Bolmont, T., Prokop, S., Winkelmann, G., Kaeser, S. A., … Jucker, M. (2009). Formation and maintenance of Alzheimer's disease β-amyloid plaques in the absence of microglia. *Nature Neuroscience*, *12*(11), 1361–1363. https://doi.org/10.1038/nn.2432

Hanisch, U.-K., & Kettenmann, H. (2007). Microglia: active sensor and versatile effector cells in the normal and pathologic brain. *Nature Neuroscience*, *10*(11), 1387–1394. https://doi.org/10.1038/nn1997

Hayley, S., Mangano, E., Strickland, M., & Anisman, H. (2008). Lipopolysaccharide and a social stressor influence behaviour, corticosterone and cytokine levels: Divergent actions in cyclooxygenase-2 deficient mice and wild type controls. *Journal of Neuroimmunology*, *197*(1), 29–36. https://doi.org/10.1016/j.jneuroim.2008.03.015

Heldmann, U., Mine, Y., Kokaia, Z., Ekdahl, C. T., & Lindvall, O. (2011). Selective depletion of Mac-1-expressing microglia in rat subventricular zone does not alter neurogenic response early after stroke. *Experimental Neurology*, *229*(2), 391–398. https://doi.org/10.1016/j.expneurol.2011.03.005

Heppner, F. L., Greter, M., Marino, D., Falsig, J., Raivich, G., Hövelmeyer, N., … Aguzzi, A. (2005). Experimental autoimmune encephalomyelitis repressed by microglial paralysis. *Nature Medicine*, *11*(2), 146–152. https://doi.org/10.1038/nm1177

Holness, C. L., & Simmons, D. L. (1993). Molecular cloning of CD68, a human macrophage marker related to lysosomal glycoproteins. *Blood*, *81*(6), 1607–1613.

Hu, X., Zhang, D., Pang, H., Caudle, W. M., Li, Y., Gao, H., … Hong, J.-S. (2008). Macrophage Antigen Complex-1 Mediates Reactive Microgliosis and Progressive Dopaminergic Neurodegeneration in the MPTP Model of Parkinson's Disease. *Journal of Immunology (Baltimore, Md. : 1950)*, *181*(10), 7194.

Hughes, T. A., Ross, H. F., Musa, S., Bhattacherjee, S., Nathan, R. N., Mindham, R. H., & Spokes, E. G. (2000). A 10-year study of the incidence of and factors predicting dementia in Parkinson's disease. *Neurology*, *54*(8), 1596–1602.

Imai, Y., & Kohsaka, S. (2002). Intracellular signaling in M-CSF-induced microglia activation: role of Iba1. *Glia*, *40*(2), 164–174. https://doi.org/10.1002/glia.10149

Jaiswal, J. K., Mattoussi, H., Mauro, J. M., & Simon, S. M. (2003). Long-term multiple color imaging of live cells using quantum dot bioconjugates. *Nature Biotechnology*, *21*(1), 47–51. https://doi.org/10.1038/nbt767

Jaiswal, J. K., & Simon, S. M. (2004). Potentials and pitfalls of fluorescent quantum dots for biological imaging. *Trends in Cell Biology*, *14*(9), 497–504. https://doi.org/10.1016/j.tcb.2004.07.012

Kierdorf, K., Erny, D., Goldmann, T., Sander, V., Schulz, C., Perdiguero, E. G., … Prinz, M. (2013). Microglia emerge from erythromyeloid precursors via Pu.1- and Irf8-dependent pathways. *Nature Neuroscience*, *16*(3), 273–280. https://doi.org/10.1038/nn.3318

Kim, W.-G., Mohney, R. P., Wilson, B., Jeohn, G.-H., Liu, B., & Hong, J.-S. (2000). Regional difference in susceptibility to lipopolysaccharide-induced neurotoxicity in the rat brain: role of microglia. *Journal of Neuroscience*, *20*(16), 6309–6316.

Klockgether, T. (2004). Parkinson's disease: clinical aspects. *Cell and Tissue Research*, *318*(1), 115–120. https://doi.org/10.1007/s00441-004-0975-6

Koprich, J. B., Reske-Nielsen, C., Mithal, P., & Isacson, O. (2008). Neuroinflammation mediated by IL-1β increases susceptibility of dopamine neurons to degeneration in an animal model of Parkinson's disease. *Journal of Neuroinflammation*, *5*(1), 8. https://doi.org/10.1186/1742-2094-5-8

Kreutzberg, G. W. (1996). Microglia: a sensor for pathological events in the CNS. *Trends in Neurosciences*, *19*(8), 312–318. https://doi.org/10.1016/0166-2236(96)10049-7

Lang, A. E., & Lozano, A. M. (1998). Parkinson's Disease. *New England Journal of Medicine*, *339*(15), 1044–1053. https://doi.org/10.1056/NEJM199810083391506

Litteljohn, D., Mangano, E., Clarke, M., Bobyn, J., Moloney, K., & Hayley, S. (2010). Inflammatory Mechanisms of Neurodegeneration in Toxin-Based Models of Parkinson's Disease. *Parkinson's Disease*, *2011*, e713517. https://doi.org/10.4061/2011/713517

Litteljohn, D., Nelson, E., Bethune, C., & Hayley, S. (2011). The effects of paraquat on regional brain neurotransmitter activity, hippocampal BDNF and behavioural function in female mice. *Neuroscience Letters*, *502*(3), 186–191. https://doi.org/10.1016/j.neulet.2011.07.041

Lotharius, J., & Brundin, P. (2002). Pathogenesis of parkinson's disease: dopamine, vesicles and α-synuclein. *Nature Reviews Neuroscience*, *3*(12), 932–942. https://doi.org/10.1038/nrn983

Lull, M. E., & Block, M. L. (2010). Microglial Activation and Chronic Neurodegeneration. *Neurotherapeutics*, *7*(4), 354–365. https://doi.org/10.1016/j.nurt.2010.05.014

Mangano, E. N., & Hayley, S. (2009). Inflammatory priming of the substantia nigra influences the impact of later paraquat exposure: Neuroimmune sensitization of neurodegeneration. *Neurobiology of Aging*, *30*(9), 1361–1378. https://doi.org/10.1016/j.neurobiolaging.2007.11.020

Mastroeni, D., Grover, A., Leonard, B., Joyce, J. N., Coleman, P. D., Kozik, B., … Rogers, J. (2009). Microglial responses to dopamine in a cell culture model of Parkinson's disease. *Neurobiology of Aging*, *30*(11), 1805. https://doi.org/10.1016/j.neurobiolaging.2008.01.001

McKercher, S. R., Torbett, B. E., Anderson, K. L., Henkel, G. W., Vestal, D. J., Baribault, H., … Maki, R. A. (1996). Targeted disruption of the PU.1 gene results in multiple hematopoietic abnormalities. *The EMBO Journal*, *15*(20), 5647.

Minami, S. S., Sun, B., Popat, K., Kauppinen, T., Pleiss, M., Zhou, Y., … Gan, L. (2012a). Selective targeting of microglia by quantum dots. *Journal of Neuroinflammation*, *9*, 22. https://doi.org/10.1186/1742-2094-9-22

Montero, M., González, B., & Zimmer, J. (2009). Immunotoxic depletion of microglia in mouse hippocampal slice cultures enhances ischemia-like neurodegeneration. *Brain Research*, *1291*, 140–152. https://doi.org/10.1016/j.brainres.2009.06.097

Paolicelli, R. C., Bolasco, G., Pagani, F., Maggi, L., Scianni, M., Panzanelli, P., … Gross, C. T. (2011). Synaptic Pruning by Microglia Is Necessary for Normal Brain Development. *Science*, *333*(6048), 1456–1458. https://doi.org/10.1126/science.1202529

Parkhurst, C. N., Yang, G., Ninan, I., Savas, J. N., Yates, J. R., Lafaille, J. J., … Gan, W.-B. (2013). Microglia promote learning-dependent synapse formation through brain-derived neurotrophic factor. *Cell*, *155*(7), 1596–1609. https://doi.org/10.1016/j.cell.2013.11.030

Peterson, A. L., & Nutt, J. G. (2008). Treatment of Parkinson's disease with trophic factors. *Neurotherapeutics*, *5*(2), 270–280. https://doi.org/10.1016/j.nurt.2008.02.003

Pissadaki, E. K., & Bolam, J. P. (2013). The energy cost of action potential propagation in dopamine neurons: clues to susceptibility in Parkinson's disease. *Frontiers in Computational Neuroscience*, *7*. https://doi.org/10.3389/fncom.2013.00013

Qin, L., Wu, X., Block, M. L., Liu, Y., Breese, G. R., Hong, J.-S., … Crews, F. T. (2007). Systemic LPS causes chronic neuroinflammation and progressive neurodegeneration. *Glia*, *55*(5), 453–462. https://doi.org/10.1002/glia.20467

Ransohoff, R. M., & Perry, V. H. (2009). Microglial Physiology: Unique Stimuli, Specialized Responses. *Annual Review of Immunology*, *27*(1), 119–145. https://doi.org/10.1146/annurev.immunol.021908.132528

Santanché, S., Bellelli, A., & Brunori, M. (1997). The Unusual Stability of Saporin, a Candidate for the Synthesis of Immunotoxins. *Biochemical and Biophysical Research Communications*, *234*(1), 129–132. https://doi.org/10.1006/bbrc.1997.6597

Schafer, D. P., Lehrman, E. K., Kautzman, A. G., Koyama, R., Mardinly, A. R., Yamasaki, R., … Stevens, B. (2012). Microglia Sculpt Postnatal Neural Circuits in an Activity and Complement-Dependent Manner. *Neuron*, *74*(4), 691–705. https://doi.org/10.1016/j.neuron.2012.03.026

Schober, A. (2004). Classic toxin-induced animal models of Parkinson's disease: 6-OHDA and MPTP. *Cell and Tissue Research*, *318*(1), 215–224. https://doi.org/10.1007/s00441-004-0938-y

Scott, E. W., Simon, M. C., Anastasi, J., & Singh, H. (1994). Requirement of transcription factor PU.1 in the development of multiple hematopoietic lineages. *Science*, *265*(5178), 1573–1577. https://doi.org/10.1126/science.8079170

Squarzoni, P., Oller, G., Hoeffel, G., Pont-Lezica, L., Rostaing, P., Low, D., … Garel, S. (2014). Microglia Modulate Wiring of the Embryonic Forebrain. *Cell Reports*, *8*(5), 1271–1279. https://doi.org/10.1016/j.celrep.2014.07.042

Stirpe, F. (2004). Ribosome-inactivating proteins. *Toxicon*, *44*(4), 371–383. https://doi.org/10.1016/j.toxicon.2004.05.004

Streit, W. J., Walter, S. A., & Pennell, N. A. (1999). Reactive microgliosis. *Progress in Neurobiology*, *57*(6), 563–581. https://doi.org/10.1016/S0301-0082(98)00069-0

Suzuki, H., Imai, F., Kanno, T., & Sawada, M. (2001). Preservation of neurotrophin expression in microglia that migrate into the gerbil's brain across the blood–brain barrier. *Neuroscience Letters*, *312*(2), 95–98. https://doi.org/10.1016/S0304-3940(01)02198-X

Takeshita, Y., & Ransohoff, R. M. (2012). Inflammatory cell trafficking across the blood-brain barrier (BBB): Chemokine regulation and in vitro models. *Immunological Reviews*, *248*(1), 228–239. https://doi.org/10.1111/j.1600-065X.2012.01127.x

Voura, E. B., Jaiswal, J. K., Mattoussi, H., & Simon, S. M. (2004). Tracking metastatic tumor cell extravasation with quantum dot nanocrystals and fluorescence emission-scanning microscopy. *Nature Medicine*, *10*(9), 993–998. https://doi.org/10.1038/nm1096

Vu, T. Q., Maddipati, R., Blute, T. A., Nehilla, B. J., Nusblat, L., & Desai, T. A. (2005). Peptide-Conjugated Quantum Dots Activate Neuronal Receptors and Initiate Downstream Signaling of Neurite Growth. *Nano Letters*, *5*(4), 603–607. https://doi.org/10.1021/nl047977c

Waisman, A., Ginhoux, F., Greter, M., & Bruttger, J. (2015). Homeostasis of Microglia in the Adult Brain: Review of Novel Microglia Depletion Systems. *Trends in Immunology*, *36*(10), 625–636. https://doi.org/10.1016/j.it.2015.08.005

Wake, H., Moorhouse, A. J., Jinno, S., Kohsaka, S., & Nabekura, J. (2009). Resting Microglia Directly Monitor the Functional State of Synapses In Vivo and Determine the Fate of Ischemic Terminals. *The Journal of Neuroscience*, *29*(13), 3974–3980. https://doi.org/10.1523/JNEUROSCI.4363-08.2009

Wu, D. C., Jackson-Lewis, V., Vila, M., Tieu, K., Teismann, P., Vadseth, C., … Przedborski, S. (2002). Blockade of Microglial Activation Is Neuroprotective in the 1-Methyl-4-Phenyl-1,2,3,6-Tetrahydropyridine Mouse Model of Parkinson Disease. *Journal of Neuroscience*, *22*(5), 1763–1771.

Yao, Y., Echeverry, S., Shi, X. Q., Yang, M., Yang, Q. Z., Wang, G. Y. F., … Zhang, J. (2016). Dynamics of spinal microglia repopulation following an acute depletion. *Scientific Reports*, *6*, 22839. https://doi.org/10.1038/srep22839

Yona, S., Kim, K.-W., Wolf, Y., Mildner, A., Varol, D., Breker, M., … Jung, S. (2013). Fate Mapping Reveals Origins and Dynamics of Monocytes and Tissue Macrophages under Homeostasis. *Immunity*, *38*(1), 79–91. https://doi.org/10.1016/j.immuni.2012.12.001

Zhan, Y., Paolicelli, R. C., Sforazzini, F., Weinhard, L., Bolasco, G., Pagani, F., … Gross, C. T. (2014). Deficient neuron-microglia signaling results in impaired functional brain

connectivity and social behavior. *Nature Neuroscience*, *17*(3), 400–406. https://doi.org/10.1038/nn.3641